THE UNIFORMITY OF DISCHARGE THROUGH MANIFOLD PIPE

by

STRONG CHIEU-HSIUNG CHUANG

B. S., National Taiwan University, 1964

A MASTER'S THESIS

submitted in partial fulfillment of the

requirements for the degree

MASTER OF SCIENCE

Department of Civil Engineering

KANSAS STATE UNIVERSITY
Manhattan, Kansas

1967

Approved by:

Richard M. Haynie
Major Professor

LD
2668
T4
1967
C55
c.2
Document

TABLE OF CONTENTS

INTRODUCTION

Manifold problems are encountered very often in engineering fields, such as: (1) control of circulation around aircraft wings and gas turbine blades by ejecting air from an aerofoil into the main stream, (2) in gas burners, or in manifolds supplying multi-cylinder internal combustion engines, (3) some irrigational facilities or grass sprayer with multiple openings along the length of the main pipe, (4) in water works processing unites such as the entrance of settling basins or back wash water distribution system of rapid sand filters, (5) pressure filters used in waterworks practice, and hot-water heating systems where a large number of radiators are connected to one header, (6) in locks for shipping, so that the rate of filling shall be evenly spread along the length of the lock since this will assist in preventing excessive movements and stresses in the mooring ropes and cables of vessels inside the lock.

Manifold problems which are likely to be of concern may be classified briefly as: (1) those with variations of pressure along the main of manifold pipe, (2) those with variations of discharge quantity along the length of manifold pipe, (3) equalizing the velocity of efflux, rather than attempting to obtain uniform quantity characteristics in order to prevent scouring effect when the scour at the orifice outlet is of concern.

There are two kinds of manifold flow phenomena: (1) Flowing manifold, the fluid is flowing out from the side ports of manifold pipe such as line source. (2) Sucking manifold, the reverse function of the blowing manifold such as line sink. The blowing manifold is more common.

If the total area of side opening is small in relation to the cross sectional area of the main pipe, then approximately equal distribution of discharge fluid may be secured from a perforated pipe with holes of equal size and equal spacing.

In general, the head loss due to friction causes the pressure head to decrease gradually along the direction of flow, while pressure recovery due to decrease of the flow velocity causes the pressure head to increase gradually along the direction of flow. In the attempt to keep discharge uniform along the manifold pipe, it is impossible to make the pressure loss and pressure gain compensate for each other, since the variation of pressure loss and pressure gain are of different characteristics. Therefore, in order to keep the discharge quantity constant along the length, several methods have been established such as: (1) Varying the size of the side openings while keeping a constant pitch for the holes. (2) Altering the pitch of the holes while retaining a constant size of side opening. (3) Varying the cross sectional area of the main pipe along its length.

The objectives of this thesis were: (1) Determine the manifold port distribution (with constant cross sectional area of the main pipe and with the same opening of the ports, the spacing between ports is varied.) and thus to provide for uniform flow distribution along the length of manifold pipe. (2) To change the pressure head at the entrance of the manifold pipe and observe the variation in the uniformity and constancy of the discharge.

THEORETICAL BASIS

Consider a straight pipe with an uniform cross sectional area, A, with discharge Q flowing in the pipe. Assume that the number of side openings of the manifold pipe is very large so that they can be considered as a long, narrow slot and fluid is flowing uniformly from the slot along the pipe. (fig. 1). If the velocity at **b**, the entrance of the pipe, is V_b then $V_b = Q/A$. Let **c** denote the closed end, so that V_c is equal to zero. Moreover, since Q is being discharged uniformly along the slot of length L, the discharge per unit length is $q = Q/L$. At some distance x downstream, the velocity in the main pipe V_x is $(Q-qx)/A$ or $(Q/A)(1-x/L)$ or $V_b(1-x/L)$.

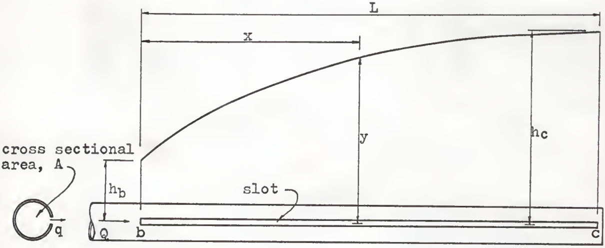

Fig. 1. Pressure Distribution Along a Slotted Manifold Pipe

Let y denote the piezometric head on the pipe at distance x downstream of b. Neglecting the friction loss, from Bernoulli equation we get

$$h_b + \frac{V_b^2}{2g} = y + \frac{V_x^2}{2g} = y + \frac{V_b^2(1-2x/L + x^2/L^2)}{2g}$$

simplifying the above relation and solving for y

$$y = h_b + \frac{V_b^2}{2g}(2x/L - x^2/L^2) \qquad (1)$$

So, y is a quadratic function of x, which means the hydraulic gradient along the manifold pipe is a parabolic curve. When x=L, $y=h_c$, so

$$h_c = h_b + \frac{V_b^2}{2g} \qquad (2)$$

Practically, when the quantity of discharge is large, i.e. V_b is relatively large, the head loss due to the frictional effect of the inner pipe surface will be pronounced. For the fully developed turbulent flow, the head loss per unit length is proportional to some power of the velocity, expressed by $h_f = KV^m$. m varies from 1.75 to 2. Darcy used m equal to 2, William-Hazen used m equal to 1.85, and Scoby used m equal to 1.9. For the case of laminar flow, by means of mathematical derivation, Hagen-Poiseuilles cited m equal to 1.

The velocity in the pipe is decreasing linearly from V_b at **b** to $V_c = 0$ at **c**. At the very downstream end where the velocity is very small flow changes from turbulent to the laminar state. Fortunately, in this experiment, the state of laminar flow occurred only at a very small length of pipe near the closed end. Therefore, it was safe to assume that turbulent flow occurred over the whole length of the pipe.

Assume m = 2, and apply the Darcy Equation

$$h_f = f\,\frac{L}{D}\,\frac{V^2}{2g}$$

From fig. 2, at the distance x from **b**, $V_x = V_b(1 - x/L)$. Head loss dh_f within the small distance dx is

$$dh_f = f_x \frac{dx}{D}\,\frac{V_b^2(1-x/L)^2}{2g} = \frac{f_x V_b^2}{2gD}(1-x/L)^2 dx \qquad (3)$$

Total head loss from **b** to x is

$$(h_f)_x = \int_0^x \frac{f_x V_b^2 (1 - x/L)^2}{2gD}\, dx$$

if f_x is constant, say f, along the whole length of L, then the above expression can be integrated as

$$(h_f)_x = \frac{fV_b^2}{2gD}(x - x^2/L + x^3/3L^2) \tag{4}$$

From equation (4), the expression of head loss is a third power function of x. Comparing equation (4) with equation (1), it is evident that two equations are of a different type, so, it is impossible to make the loss of head and recovery of head compensate for each other. When x = L, then

$$(h_f)_c = \frac{fV_b^2 L}{6gD} \tag{5}$$

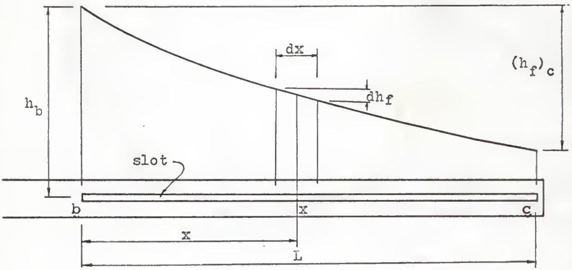

Fig. 2. Friction Head Loss Along a Slotted Manifold Pipe

Consequently, the actual head along the manifold pipe can be obtained by subtracting equation (4) from equation (1).

$$h_x = y - (h_f)_x = h_b + \frac{V_b^2}{2g}(2x/L - x^2/L^2) - \frac{fV_b^2}{2gD}(x - x^2/L + x^3/3L^2)$$

$$\therefore \quad h_x = h_b + \frac{V_b^2}{2g}\left[(2/L - f/D)x + (f/LD - 1/L^2)x^2 - \frac{fx^3}{3L^2D} \right] \qquad (6)$$

In viewing equation (6), it is easy to show that it is impossible to maintain h_x constant along L. To prove this, put $h_x = h_b$, then $(2/L - f/D)x + (f/LD - 1/L^2)x^2 - (f/3L^2D)x^3 = 0$, one and only one condition to get this result is that all the coefficients be equal to zero, and this is not practical.

Equation (6) is approximately true only for the case of manifold pipes with an open end so that the variation of the velocity from b to c is small and f remains approximately constant over the whole manifold length. For the closed end manifold pipe, f varies with the Reynolds Number and equation (6) cannot be used. It is, therefore, necessary to develop another method to determine the pressure distribution.

Divide the manifold pipe into N equal subdivisions with the length of each subdivision L/N. Assume the velocity is constant within each subdivision as shown on fig. 3.

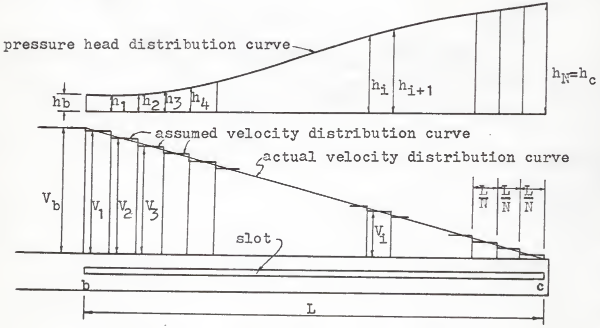

Fig. 3. Pressure Head and Velocity Distribution Curves Along a Slotted Manifold Pipe.

From equation (3), in each subdivision

$$(dh_f)_1 = \frac{f_1 V_b^2 (L/N)}{2gD}\left(\frac{N-1}{N}\right)^2$$

$$(dh_f)_2 = \frac{f_2 V_b^2 (L/N)}{2gD}\left(\frac{N-2}{N}\right)^2$$

....

$$(dh_f)_i = \frac{f_i V_b^2 (L/N)}{2gD}\left(\frac{N-i}{N}\right)^2$$

$$\therefore \quad (h_f)_i = (dh_f)_1 + (dh_f)_2 + \dots + (dh_f)_i$$

$$= \sum_{i=1}^{i=i} \frac{f_i V_b^2 (L/N)}{2gD}\left(\frac{N-i}{N}\right)^2$$

$$\therefore \quad h_i = y_i - (h_f)_i$$

From equation (1) $y_i = h_b + \frac{V_b^2}{2g}(2i/N - i^2/N^2)$

$$\therefore \quad h_i = h_b + \frac{V_b^2}{2g}\left[2i/N - (i/N)^2 - \sum_{i=1}^{i=i} \frac{f_i (L/N)}{D}\left(\frac{N-i}{N}\right)^2\right] \tag{7}$$

Based on equation (7), the head distribution curves of various discharge, Q, flowing in a two inches PVC pipe have been ploted in fig. 15.

So far it has been assumed that the manifold openings were so numerous that they could be regarded as a slot extending continuously along the length L. Actually, the opening was discontinuous and when fluid passed through each of the side openings it caused a certain head loss. This type of problem has been extensively studied. Zenze[1] presented an empirical rule, (Fig.4), whereby the pressure difference between 1 and 2, P_{1-2}, and 1 and 3, P_{1-3}, can be expressed empirically

$$P_{1-2} = 0.000135(1.36V_2^2 - 0.64V_1^2 - 0.72V_1V_2) \tag{8}$$

$$P_{1-3} = 0.000135(1.8V_3^2 - 0.368V_1V_2) \tag{9}$$

En-Yun Hsu[2] presented an entirely different type of analysis. He used the free streamline theory in determining the principal character of the lateral efflux. Considering the efflux from a circular orifice in a circular manifold pipe as type of irrotational two dimensional branching flow, a relationship was derived

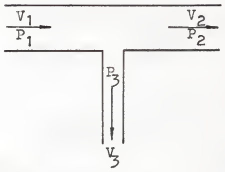

Fig. 4

by means of the method of successive conformal transformation for the theoretical coefficient of contraction for two dimensional lateral efflux. With reference to fig. 5, the relationship,

$$C_i = F\left(\frac{V_{i+1}}{V_i}, \frac{a}{A}\right) \tag{10}$$

was defined in general but implicit form. Equation (10) is applicable to the dividing flow with the provisions that (1) the ratio of the area of the lateral to the area of the main conduit be the same in each case, and (2) the energy loss is like that in an abrupt expansion

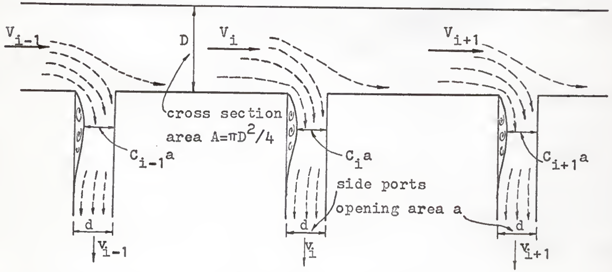

Fig. 5

Flow Contraction at Manifold Side Ports

downstream from a section at which the contraction of the jet can be assumed essentially complete. Thus, the energy loss, h_f, of fluid by passing through the side ports is computed from the known formula for head loss at a boundary enlargement,

$$h_f' = \frac{(V_i' - V_i)^2}{2g}$$

where V_i' is the velocity at the contracted section. Simplified to dimensionless form

$$\frac{h_f'}{\frac{V_i^2}{2g}} = \left(\frac{1}{C_i} - 1\right)^2$$

The representative curve of C_i is reproduced as fig. 6.

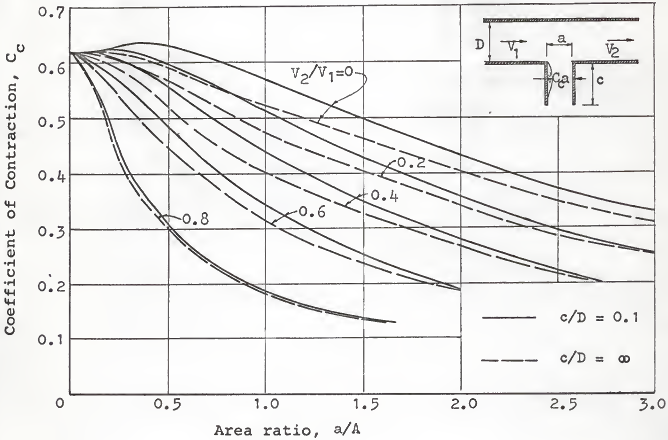

Fig. 6

Coefficient of Contraction Versus Area Ratio Curve
With Velocity Ratio as a Third Parameter.

PRELIMINARY STUDIES

The experiment was carried out by using a two inches PVC pipe as the main pipe. Although the nominal size was two inches, the actual inner diameter was 2.193 inches. The size of side opening was 19/32 inches in diameter and connected with a tube two inches in length as a flow guide to prevent flow from slanting forward in the direction of main pipe flow. Two essential items of information had to be known before starting to design the manifold system. They are skin friction coefficient, f, of the two inches PVC pipe and the discharge coefficient C_q, of the side ports.

(1) Determination of f-curve in terms of the Reynold's Number:

The experimental apparatus is shown schematically in fig. 7. e is a control valve, k is the orifice connected to a manometer with mercury as the indicating fluid. The detail structure of the orifice

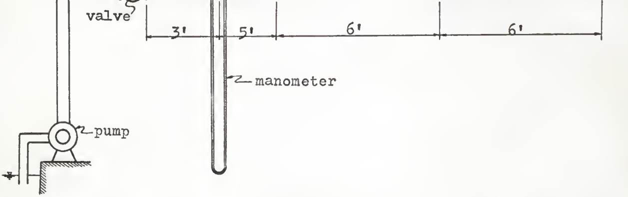

Fig. 7

Experimental Apparatus for Determining Pipe Friction Factor

and manometer is shown in fig. 8. A distance of 5 feet downstream from k to b was provided as a calming length. The loss of head from b to d and from d to c can be read from the plastic tubes which were placed at positions b, d, and c. d was the mid-point of length bc.

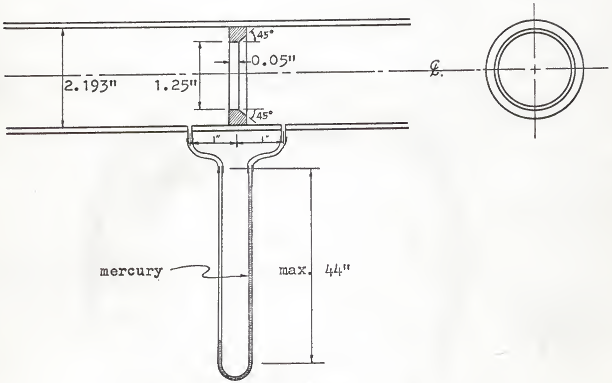

Fig. 8. Orifice Plate and Manometer

The orifice was calibrated and the results are shown in fig. 9. The quantity of discharge can be determined by reading the head difference of the manometer and then obtaining the corresponding discharge from fig. 9.

By the Darcy Equation $h_f = f(L/D)(V^2/2g)$, where h_f is the head loss in the distance L, D is pipe diameter, V is mean velocity of the pipe flow. Solving for the friction factor it is found $f=(2gDh_f)/(LV^2) = (\pi^2 gD^5 h_f)/(8LQ^2)$. Since D = 2.193", and L = 12', then

$$f = 6.75(10^{-3})(hf/Q^2) \tag{11}$$

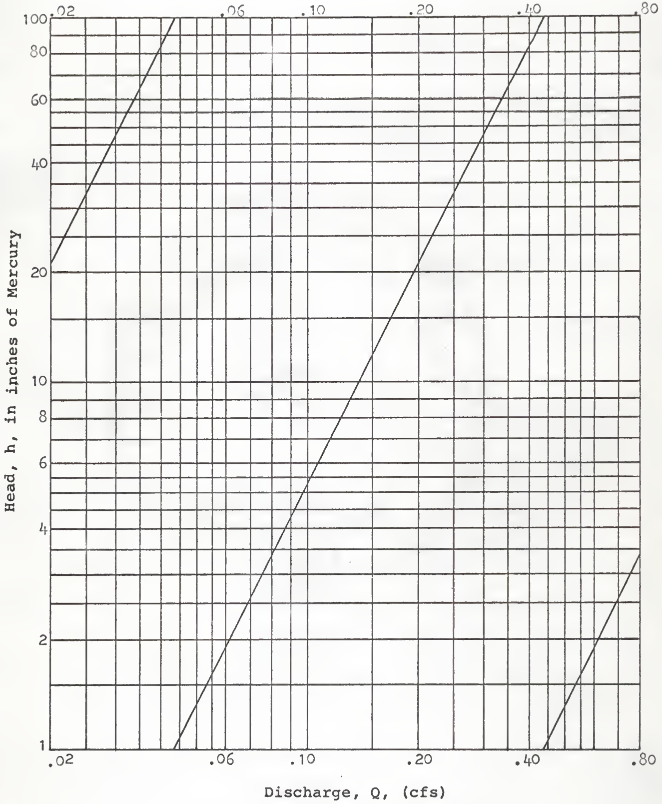

Fig. 9. Orifice Calibration Curve

Moreover the Reynold's Number, $N_r = (VD)/\nu = (4Q)/(\pi D \nu)$. For a temperature equal to 70°F, $\nu = 1.05(10^{-5})$ ft^2/sec. So that

$$N_r = 6.64(10^5)Q. \tag{12}$$

From equations (11) and (12), it was necessary to measure only h_f and Q, then it was able to plot a curve of f vs N_r.

The total number of testing points were fifty three. The data of the test are presented in appendix A. The test range was from a Reynold's Number of $4(10^3)$ to $6.6(10^4)$. The resulting Stanton curve (f vs N_r curve) is plotted in fig. 11. The curve of Blasiu's equation $f = 0.3164/N_r^{0.25}$ for smooth pipe is also plotted for the purpose of comparison.

(2) Determination of the discharge coefficient of orifice:

The coefficient of discharge is defined as

$$C_q = \frac{Q_3}{a\sqrt{2gh}}$$

The detail of the side opening is shown in fig. 10

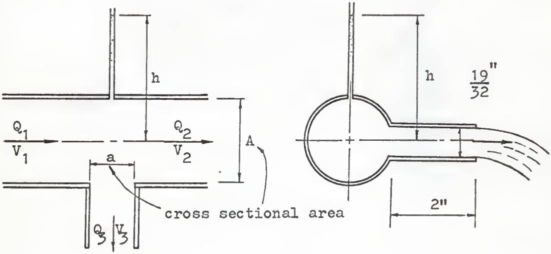

Fig. 10. Detail of Manifold Side Port

According to Zenz[1] and En-Yun Hsu[2] C_q is a function of Q_2/Q_1 and

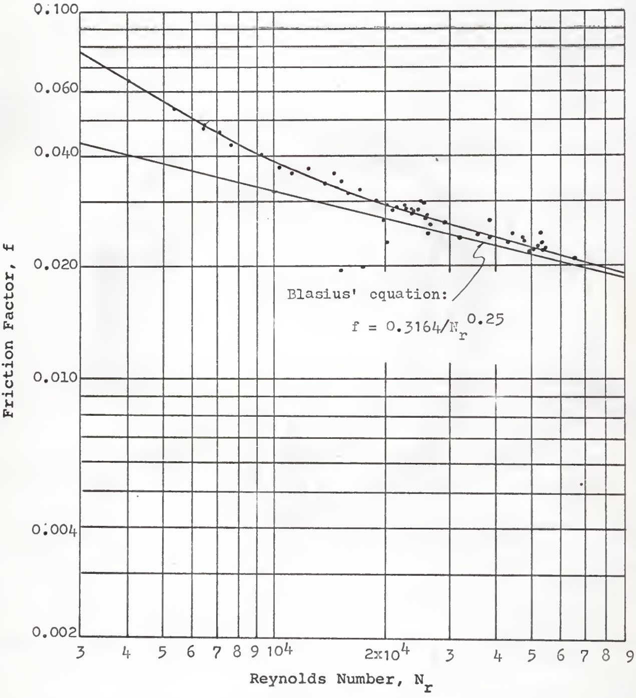

Fig. 11. Stanton curve of 2 inches PVC pipe.

a/A. Now $a/A = (d/D)^2 = 0.0737$ is a constant value for each side port. The only dependent variable is Q_2/Q_1 or V_2/V_1. In order to determine a C_q vs V_2/V_1 curve, one typical side port was taken as a test orifice. The experiment of determining C_q is shown on fig. 12, where Q_i was read from manometer, q was determined by direct measuring, $Q_{i+1}=Q_i-q$

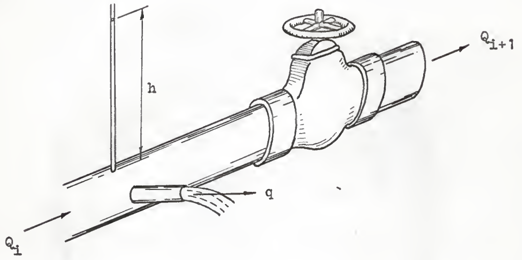

Fig. 12. Pictorial Sketch of Manifold Section

then can be obtained. Hence $Q_{i+1}/Q_i = V_{i+1}/V_i$ curve was determined. one can then compute $C_q = q/(a\sqrt{2gh})$. The C_q vs V_{i+1}/V_i curve is shown in fig. 13. The experimental data are presented in appendix B.

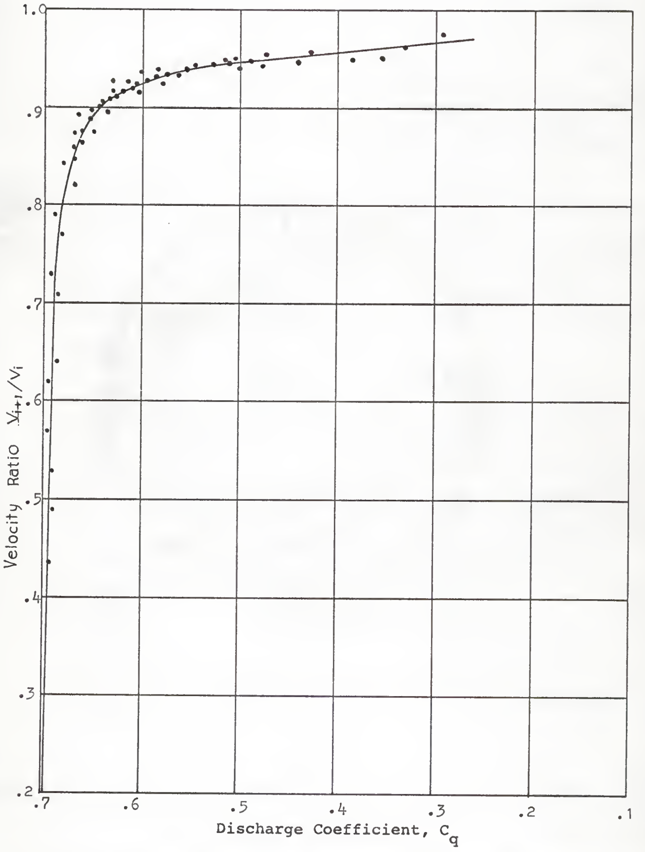

Fig. 13. Velocity Ratio Versus Side Port Discharge Coefficient

DESIGN OF THE EXPERIMENTAL APPARATUS

Let D: Denote diameter of main pipe = 2.193 inches.

A: Cross sectional area of main pipe = 0.02622 sq. ft.

d: Diameter of the opening ports of the manifold pipe = $\frac{19''}{32}$

a: Cross sectional area of each of the side opening = 0.00195 sq. ft..

n: Total number of openings within the manifold length L.

Q: Total discharge at the inlet of the manifold pipe=0.25 cfs.

q: Uniform discharge per unit length of manifold pipe equal to Q/L = 0.0208 cfs/ft.

q_i:Discharge through ith port of opening.

h_b: Water head at the entrance of the manifold.

h_c: Water head at the dead end of the manifold = 20 inches.

Now if keep D, L, Q, h_b (and hence h_c) constant, then n and d will depend on each other. The purpose of this experiment was to determine the value of n, and the spacing between these n openings while keeping D, d, L, h_b, and h_c constant and suppling a certain designated Q.

From the analysis given on pages 6 and 7, assume N=20, the pressure head distribution along the manifold pipe was obtained by the calculation shown in table 1, where

column (1) (L-x)/L is equivalent to (N-i)/N = 1-i/20, i from 1 to 20.

column (2) $Q_i = Q(N-i)/N = 0.0125(N-i)$.

column (3) $V_i = Q_i/A = Q_i/0.02622 = 0.476(20-i)$.

column (6) $N_r = V_iD/\nu = 1.74(10^4)V_i$.

column (7) skin friction coefficients, f, were obtained from fig. 11.

column (8) Δh were computed from equation (3) where dx is equal to 0.6 ft..

column (9) summation of column (8).

column(10) column (5) minus column (9), where Δh are as shown on fig. 14.

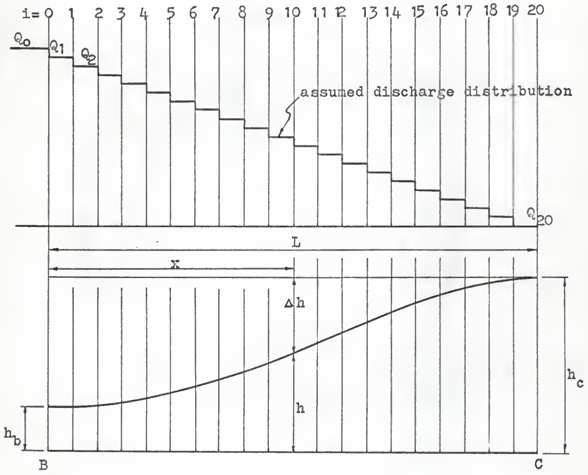

Fig. 14. Assumed Discharge and Pressure Head Distribution

From the table 1, for i=0 (at B), we see that Δh is equal to 0.734, so that $h_c - h_b = 0.734$. The "Δh curve" for Q = 0.25 cfs is plotted on fig. 15. Each quantity of Q will have a characteristic Δh curve. From fig. 15 Δh curves for different values of Q may be determined. The calculations of the Δh curves for discharges, Q,

Table 1 Computations of h-curve (Q=0.25 cfs in 2" PVC pipe).

i	$\frac{L-x}{L}$	Q_i	V_i	V_i^2	$\frac{V_i^2}{2g}$	N_r	f_x	Δh_f	$\sum h_f$	Δh
	(1)	(2)	(3)	(4)	(5)	(6)	(7)	(8)	(9)	(10)
20	-	-	-	-	-	-	-	-	-	-
19	.05	.0125	.48	.2	.004	8,300	.0425	.0005	.0005	.003
18	.10	.0250	.95	.9	.014	16,600	.0318	.0015	.0020	.012
17	.15	.0375	1.43	2.0	.032	24,900	.0276	.0029	.0049	.027
16	.20	.0500	1.91	3.6	.056	33,200	.0251	.0046	.0095	.046
15	.25	.0625	2.38	5.7	.088	41,500	.0238	.0069	.0164	.072
14	.30	.0750	2.86	8.3	.129	49,800	.0228	.0097	.0261	.103
13	.35	.0875	3.33	11.1	.173	57,100	.0221	.0126	.0387	.134
12	.40	.1000	3.81	14.5	.225	66,400	.0215	.0159	.0546	.170
11	.45	.1125	4.29	18.4	.285	74,700	.0210	.0197	.0743	.211
10	.50	.1250	4.77	22.8	.353	83,000	.0207	.0241	.0984	.255
9	.55	.1375	5.24	27.5	.427	91,300	.0205	.0288	.1272	.300
8	.60	.1500	5.72	32.7	.508	99,600	.0203	.0339	.1611	.347
7	.65	.1625	6.19	38.4	.596	107,900	.0202	.0395	.2006	.395
6	.70	.1750	6.67	44.5	.691	116,200	.0201	.0456	.2462	.445
5	.75	.1875	7.15	51.1	.793	124,500	.0201	.0524	.2986	.494
4	.80	.2000	7.63	58.2	.904	132,800	.0200	.0594	.3580	.546
3	.85	.2125	8.11	65.8	1.021	141,100	.0200	.0672	.4252	.596
2	.90	.2250	8.58	73.6	1.143	149,400	.0200	.0751	.5003	.643
1	.95	.2375	9.05	81.9	1.272	157,700	.0200	.0836	.5839	.688
0	1.00	.2500	9.53	90.8	1.411	166,000	.0200	.0928	.6767	.734

The notations of above table referred to fig. 14

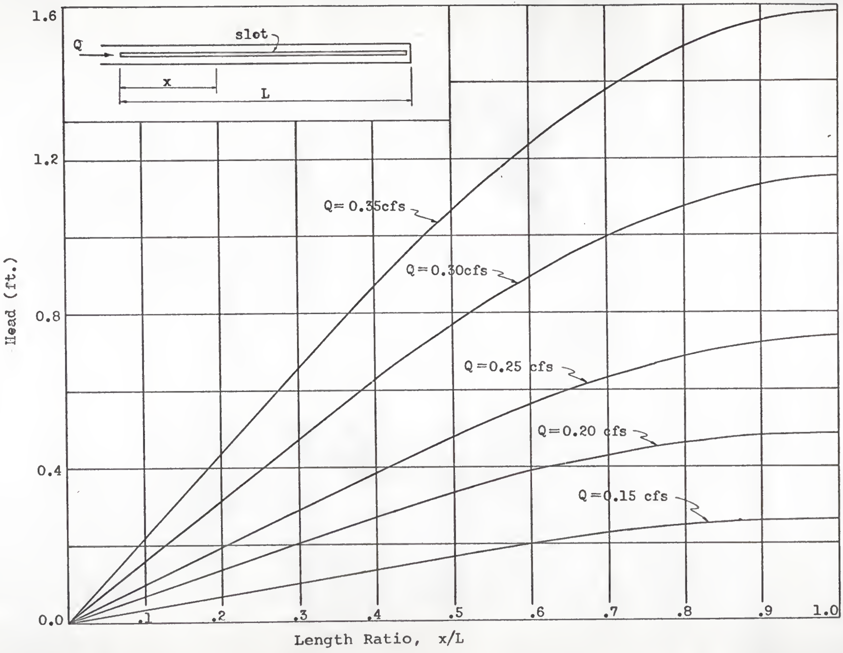

Fig. 15. Characteristic Change of Head Curve

equal to 0.15, 0.20, 0.30, 0.35 cfs were presented in appendix C.

It was also assumed that h_c= 20 inches (or 1.667 ft.), so that h_b= 1.667- 0.734 = 0.933 ft.. Based on this assumption, the distribution of pressure head along the manifold pipe is known. Since the opening area is known, and C_q can be obtained from fig. 13, and the pressure head, h, is known at each point of the length, then the corresponding $q = C_q a \sqrt{2gh}$ can be evaluated. A q-curve along the manifold pipe L can then be plotted.

The calculations are given in table 2, where

column (1) obtained from table (1).

column (2) obtained by subtracting column (1) from 1.667 ft.

column (4) a = 0.00195 sq ft., $a\sqrt{2gh}$ = 0.00195 x column (3).

column (5) calculated from column (3) of table 1.

column (6) obtained from fig. 12.

column (7) column (4) times column (6).

The resulting q-curve is shown in fig. 16.

The next step is to determine the spacing (therefore the number of side openings). From fig. 16, at the entrance, b, of the manifold pipe q=0.00696 cfs. Since the required uniform discharge is Q/L = 0.0208 cfs/ft,, the interval required between the first two ports is equal to 0.00696/0.028 = 0.334 ft to make the discharge uniform. Therefore, the second side opening was drilled at a distance of 0.334 ft from the first opening. At the second position, from fig. 16, the discharge is found to be equal to 0.00729 cfs. so that the second interval required is 0.00729/0.0208 = 0.351 ft to make the discharge uniform. Therefore the opening was drilled at a distance of 0.334 + 0.351 = 0.685 ft from the first opening. At the third position, again,

Table 2 Computation of q-curve

	(1)	(2)	(3)	(4)	(5)	(6)	(7)
i	Δh	h	$\sqrt{2gh}$	$a\sqrt{2gh}$	V_{i+1}/V_i	C_q	q
20	0.000	1.667	10.34	0.02019	0.000	0.697	0.01406
19	0.003	1.664	10.33	0.02011	0.000	0.697	0.01400
18	0.012	1.655	10.30	0.02008	0.500	0.694	0.01392
17	0.027	1.640	10.26	0.02000	0.667	0.690	0.01380
16	0.046	1.621	10.20	0.01988	0.749	0.687	0.01366
15	0.072	1.595	10.12	0.01973	0.800	0.682	0.01345
14	0.103	1.564	10.03	0.01955	0.834	0.675	0.01319
13	0.134	1.533	9.93	0.01935	0.858	0.670	0.01296
12	0.170	1.497	9.81	0.01912	0.874	0.663	0.01267
11	0.211	1.456	9.68	0.01888	0.889	0.654	0.01234
10	0.255	1.412	9.53	0.01857	0.900	0.645	0.01197
9	0.300	1.367	9.37	0.01826	0.909	0.633	0.01157
8	0.347	1.320	9.21	0.01795	0.917	0.620	0.01113
7	0.395	1.272	9.05	0.01765	0.923	0.606	0.01069
6	0.445	1.222	8.86	0.01715	0.928	0.596	0.01021
5	0.494	1.173	8.69	0.01693	0.933	0.573	0.00972
4	0.546	1.121	8.50	0.01656	0.937	0.555	0.00918
3	0.596	1.071	8.30	0.01617	0.942	0.533	0.00864
2	0.643	1.024	8.13	0.01584	0.945	0.512	0.00812
1	0.688	0.979	7.93	0.01546	0.948	0.489	0.00755
0	0.734	0.933	7.75	0.01510	0.950	0.460	0.00696

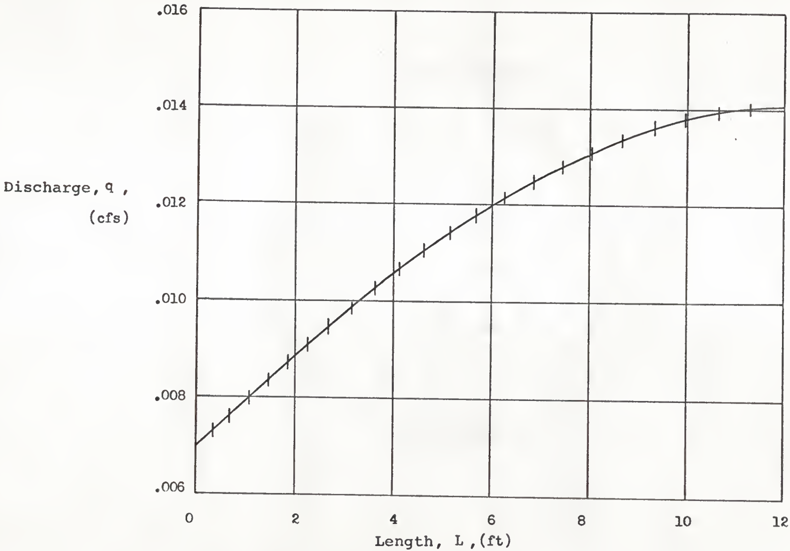

Fig. 16.

Discharge Distribution Curve

Table 3 Calculations of side opening spacing

Number of holes	q (cfs)	Spacing ft.	Spacing inches	Cumulative spacing ft.	Cumulative spacing inches
1	0.00696	0.334	4.01	0.334	4.01
2	0.00729	0.351	4.21	0.685	8.22
3	0.00763	0.367	4.40	1.052	12.62
4	0.00799	0.384	4.61	1.436	17.23
5	0.00834	0.401	4.81	1.837	22.04
6	0.00868	0.417	5.01	2.254	27.05
7	0.00905	0.435	5.23	2.689	32.28
8	0.00942	0.453	5.44	3.142	37.72
9	0.00983	0.473	5.68	3.615	43.40
10	0.01023	0.492	5.91	4.107	49.31
11	0.01062	0.511	6.13	4.618	55.44
12	0.01100	0.529	6.35	5.147	61.79
13	0.01137	0.547	6.57	5.694	68.36
14	0.01177	0.566	6.79	6.260	75.15
15	0.01213	0.583	7.00	6.843	82.15
16	0.01247	0.600	7.20	7.443	89.35
17	0.01279	0.615	7.38	8.058	96.73
18	0.01307	0.628	7.54	8.686	104.27
19	0.01332	0.641	7.69	9.327	111.96
20	0.01356	0.652	7.83	9.979	119.79
21	0.01375	0.662	7.94	10.641	127.73
22	0.01389	0.668	8.02	11.309	135.75
23	0.01400	0.673	8.08	11.982	143.83

from fig. 16, the discharge is equal to 0.00799 cfs. The intervals between outlets obtained by repeating this process are shown in table 3. The cumulative distance from the first hole to the twenty-third hole is 11.982 ft $\approx$ 12 ft.

This finishes the design of the manifold pipe. The apparatus is shown in fig. 17 with 23 side ports drilled over the length bc and the spacings are as shown in table 3.

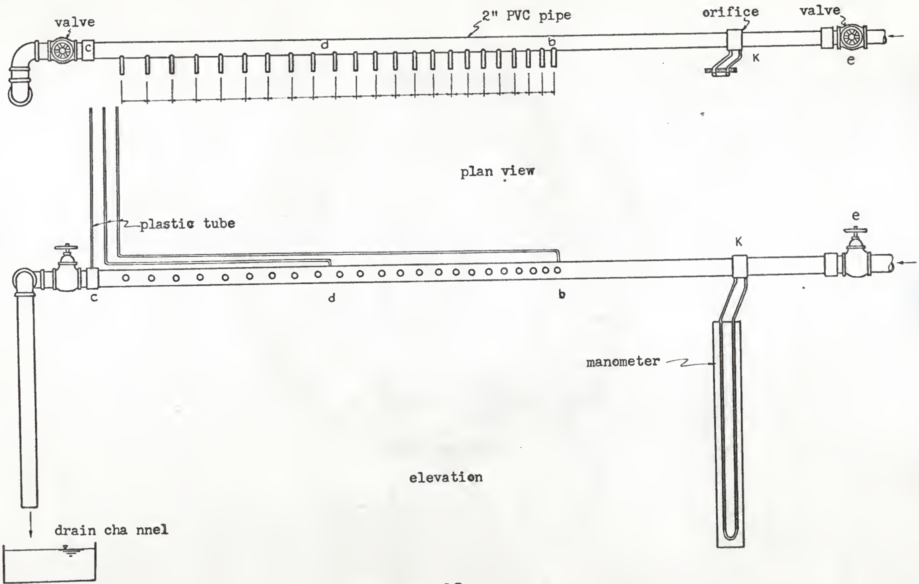

Fig. 17.

Schematic of Experimental Apparatus

EXPERIMENTAL RESULTS

The experimental apparatus is shown schematically in fig. 17. When the experiment was running, the downstream valve was closed and the upstream valve was opened. The discharge quantity, Q, was controlled by valve e and determined by means of the orifice and manometer k. The discharge through each side opening was measured by direct weighing. The sum of the discharge flowing from these twenty three openings compared favorably to the total inflow Q which was read from the manometer. This indicated that the accuracy of the measurement of the discharge through the side ports and the precision of the manometer were good.

In order to minimize the personal and the instrumental error, the experiments were repeated three times. The results of each of the tests was nearly the same. The final data of the test obtained by taking the arithmetic mean of the three tests are as presented in table 4.

When the manometer indicated that inflow, Q, was equal to 0.25 cfs, the pressure head at b, based upon the theoretical analysis, should have been 0.933 ft., at c it should have been 1.667 ft., and at d it should have been 1.564 ft.. The results as shown in table 4 indicate that h_b was equal to 0.901 ft. which is a -3.22% deviation from the theoretical value of 0.933 ft.. The head at d was equal to 1.496 ft. which is a -4.43% deviation from the theoretical value of 1.564 ft., and the head at c was equal to 1.750 ft. which is a +4.96% deviation from the theoretical value.

Table 4 also gives the discharge from each of the ports and its

Table 4

h_b=0.901 ft, h_d=1.496 ft, h_c=1.750 ft.

port no.	theoretical discharge (cfs)	experimental discharge (cfs)	deviation cfs	deviation %
1	0.00696	0.00701	+ 0.00005	+ 0.72
2	0.00729	0.00737	+ 0.00008	+ 1.10
3	0.00763	0.00778	+ 0.00015	+ 1.97
4	0.00799	0.00758	- 0.00041	- 5.13
5	0.00834	0.00807	- 0.00027	- 3.24
6	0.00868	0.00870	+ 0.00002	+ 0.23
7	0.00905	0.00903	- 0.00002	- 0.23
8	0.00942	0.00939	- 0.00003	- 0.32
9	0.00983	0.00987	+ 0.00004	+ 0.41
10	0.01023	0.00990	- 0.00033	- 3.23
11	0.01062	0.01020	- 0.00042	- 3.94
12	0.01100	0.01114	+ 0.00014	+ 1.27
13	0.01137	0.01170	+ 0.00033	+ 2.90
14	0.01177	0.01200	+ 0.00023	+ 1.95
15	0.01213	0.01228	+ 0.00015	+ 1.24
16	0.01247	0.01260	+ 0.00013	+ 1.04
17	0.01279	0.01292	+ 0.00013	+ 1.02
18	0.01307	0.01287	- 0.00020	- 1.53
19	0.01332	0.01326	- 0.00006	- 0.45
20	0.01356	0.01351	- 0.00005	- 0.37
21	0.01375	0.01381	+ 0.00006	+ 0.44
22	0.01389	0.01397	+ 0.00008	+ 0.58
23	0.01400	0.01476	+ 0.00076	+ 5.43
Σ	0.24916	0.24972	+ 0.00056	+ 1.86

Table 5

$Q = 0.25$ cfs. $q = 0.0208$ cfs/ft.

port no.	experimental discharge (cfs) (1)	ΔL (ft) (2)	uniformity q (cfs/ft) (3)	uniformity dimensionless distributions (4)
1	0.00701	0.334	0.210	1.009
2	0.00737	0.351	0.210	1.009
3	0.00778	0.367	0.212	1.018
4	0.00758	0.384	0.198	0.951
5	0.00807	0.401	0.201	0.966
6	0.00870	0.417	0.209	1.003
7	0.00903	0.435	0.207	0.994
8	0.00939	0.453	0.207	0.994
9	0.00987	0.473	0.209	1.004
10	0.00990	0.492	0.201	0.966
11	0.01020	0.511	0.200	0.961
12	0.01114	0.529	0.211	1.014
13	0.01170	0.547	0.214	1.029
14	0.01200	0.566	0.212	1.019
15	0.01228	0.583	0.211	1.014
16	0.01260	0.600	0.210	1.009
17	0.01292	0.615	0.210	1.009
18	0.01287	0.628	0.205	0.985
19	0.01326	0.641	0.207	0.995
20	0.01351	0.652	0.207	0.995
21	0.01381	0.662	0.209	1.004
22	0.01397	0.668	0.209	1.004
23	0.01476	0.673	0.219	1.052

deviation from the theoretical value. From the recorded data, it is seen that the largest error was about ± 5% and occurred at port 4 and port 23. Ports 3, 5, 10, 11, 13, 14, and 18 also had a relatively large deviation from the theoretical value. The deviations were due to the lack of skill in drilling the holes and connecting the guide tube of the side ports. This would influence the cross sectional area , a, and the discharge coefficient C_q of the side ports.

The uniformity of the test results are shown in table 5. Column (3) was obtained by dividing column (1) by column (2) and column (4) was obtained by dividing column (3) by the value of 0.0208 cfs/ft. The values in column (3) have been plotted in fig. 18. The values in column (4) have been plotted in dimensionless form in fig. 28.

All the deviations between the theoretical value and the experimental data discussed above are believed to be caused by error in the fundamental assumptions and by deviations in the design from the fundamental assumptions. The main factors which might be responsible are stated in the following.

(1) In designing this experiment apparatus, it was assumed that the pipe was divided into twenty equal subdivisions and that the discharge in each subdivision was constant as shown in column (2) of table (1). In the actual case, the manifold pipe was drilled with twenty three ports with the distance between each port varied as shown in table 3 and fig. 17. Part of the deviation between experimental and theoretical values might be attributed to this change.

(2) It was assumed that the pressure head loss in the main pipe was due only to frictional effect and momentum effect. The

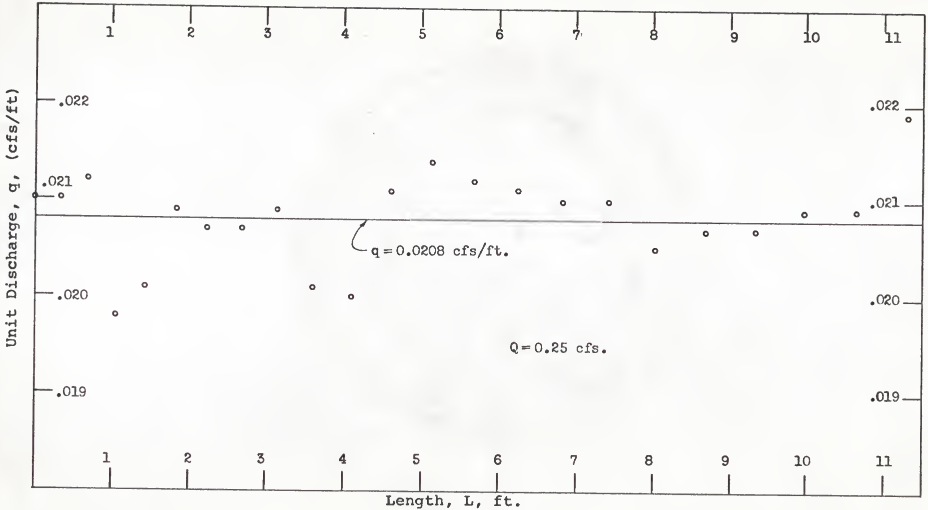

Fig. 18.

Discharge Distribution Curve

turbulence loss in the main pipe when the fluid was divided into many branches was neglected.

(3) It was found that the discharge through each of the ports was not exactly equal to the design value. Therefore, the discharge per unit length of the manifold pipe was not a constant. This effect would influence the pressure head in the pipe, and the latter will also influence the former.

In general the deviations were small, and the results revealed that the basic assumptions and the theoretical method of analysis for the design of the manifold pipe given before were fairly satisfactory.

Following the completion of the first run the inflow quantity was changed by adjusting the control valve at e, and the pressure head h_b, h_d, and h_c changed correspondingly. In general, when Q became larger, then h_b, h_c, and h_d became larger; when Q became smaller, then h_b, h_c, and h_d became smaller. The relationship between Q and h was determined and is presented in the following table

Table 6

Q (cfs)	h_b (ft)	h_d (ft)	h_c (ft)
0.07	0.021	0.083	0.109
0.10	0.088	0.169	0.213
0.13	0.211	0.362	0.445
0.16	0.365	0.608	0.722
0.19	0.540	0.872	1.026
0.22	0.709	1.183	1.418
0.25	0.901	1.483	1.726
0.28	1.167	1.917	2.250
0.31	1.488	2.375	2.719

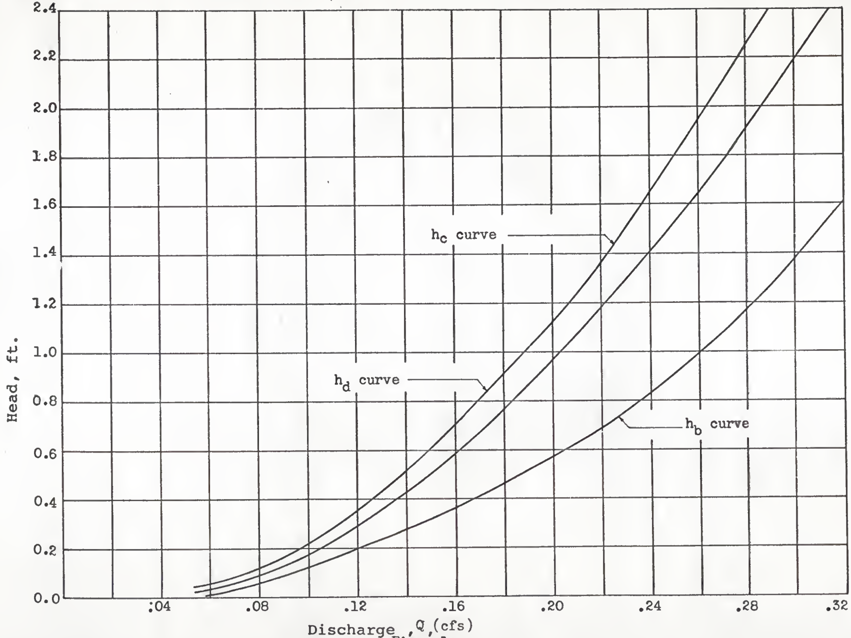

Fig. 19.
Head Versus Discharge Curves for Points, b, c, and d.

The data of table 6 have been plotted in fig. 19.

Discharges, Q, of 0.07 cfs, 0.10 cfs, 0.13 cfs, 0.16 cfs, 0.19 cfs, 0.22 cfs, 0.28 cfs, and 0.31 cfs were tested and the results are presented in tables 7 to 14. The discharge per unit length of manifold pipe for each case is plotted in fig. 20 to 27.

From these experimental results it was found that when Q was 0.25 cfs the uniformity characteristic of manifold pipe was fairly good as discussed before. When Q was gradually increased the uniformity characteristic of the manifold pipe was decreased; the discharge per unit length, q, decreased at the beginning of the manifold pipe and increased at the center portion of the manifold pipe. With Q = 0.28 cfs, table 8 and fig. 21 show that the uniformity varied from -6.3% at the entrance to +3% of the uniform q (=0.02342 cfs/ft) at the mid-portion of the manifold pipe. When the inflow Q was increased further, this tendency of nonuniformity became more pronounced. When Q = 0.3085 cfs it can be seen from table 7 and fig. 20, that the uniformity varied from -9.2% at the entrance to +4.2% of the uniform q (=0.257 cfs/ft.) at the mid-portion of the manifold pipe.

When the inflow discharge was reduced below 0.25 cfs, the manifold pipe experienced the same property of nonuniformity, but the non-uniformity was in the reverse order. When Q was greater than 0.25 cfs, the distribution curve of discharge per unit length, q, along the manifold pipe was concave downward as shown by fig. 20 and 21. When Q was smaller than 0.25 cfs the distribution curve for q was concave upward as shown by fig. 22 to 26. The q is larger at the entrance, and gradually decreases in the direction of flow. At the mid-portion of the manifold pipe the q became minimum and then increased gradually

Table 7 $Q=0.3085$cfs, $h_b=1.488$ft, $h_d=3.475$ft, $h_c=2.730$ft.

port no.	q (cfs)	ΔL (ft)	uniformity q/ΔL (cfs/ft)	dimensionless uniformity	% of deviation from uniform distribution
1	0.00786	0.334	0.235	0.914	- 8.6
2	0.00860	0.351	0.245	0.953	- 4.7
3	0.00912	0.367	0.249	0.969	- 3.1
4	0.00884	0.384	0.230	0.895	-10.5
5	0.00969	0.401	0.242	0.942	- 5.8
6	0.01050	0.417	0.252	0.981	- 1.9
7	0.01100	0.435	0.253	0.985	- 1.5
8	0.01150	0.453	0.254	0.988	- 1.2
9	0.01220	0.473	0.258	1.003	+ 0.3
10	0.01221	0.492	0.249	0.968	- 3.2
11	0.01268	0.511	0.248	0.965	- 3.5
12	0.01366	0.529	0.258	1.003	+ 0.3
13	0.01480	0.547	0.271	1.054	+ 5.4
14	0.01524	0.566	0.269	1.048	+ 4.8
15	0.01562	0.583	0.268	1.043	+ 4.3
16	0.01608	0.600	0.268	1.043	+ 4.3
17	0.01645	0.615	0.267	1.040	+ 4.0
18	0.01640	0.628	0.261	1.016	+ 1.6
19	0.01680	0.641	0.262	1.020	+ 2.0
20	0.01690	0.652	0.259	1.008	+ 0.8
21	0.01717	0.662	0.259	1.008	+ 0.8
22	0.01717	0.668	0.257	1.000	0.0
23	0.01800	0.673	0.268	1.044	+ 4.4
	0.30849				

noté : uniform q = 0.257 cfs/ft

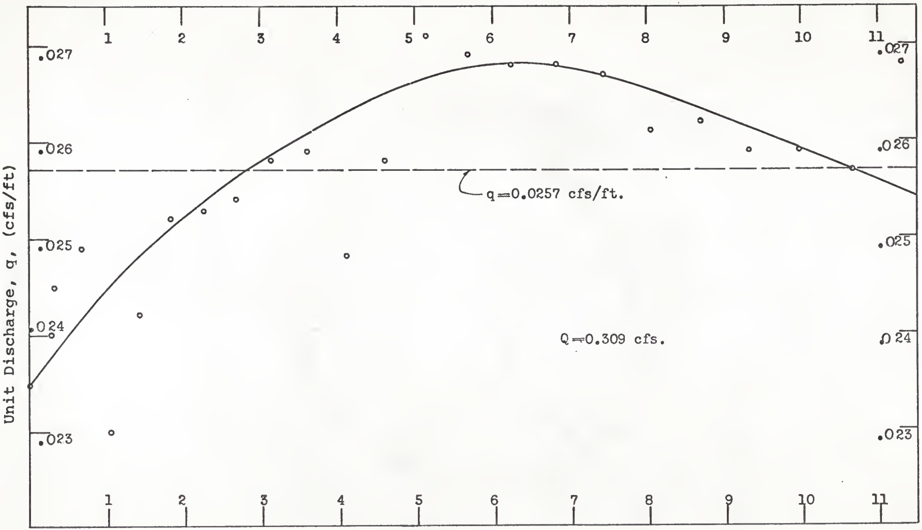

Fig. 20.

Discharge Distribution Curve

Table 8 Q=0.28074cfs, h_b=1.167ft, h_d=1.917ft, h_c=2.250ft.

port no	q (cfs)	ΔL (ft)	uniformity q/ΔL (cfs/ft)	uniformity dimensionless uniformity	uniformity % of deviation from uniform distribution
1	0.00750	0.334	0.02244	0.958	- 4.2
2	0.00796	0.351	0.02268	0.968	- 3.2
3	0.00848	0.367	0.02310	0.986	- 1.4
4	0.00823	0.384	0.02141	0.915	- 8.5
5	0.00886	0.401	0.02210	0.944	- 5.6
6	0.00957	0.417	0.02292	0.979	- 2.1
7	0.01004	0.435	0.02310	0.987	- 1.3
8	0.01050	0.453	0.02319	0.990	- 1.0
9	0.01100	0.473	0.02327	0.993	- 0.7
10	0.01110	0.492	0.02256	0.963	- 3.7
11	0.01150	0.511	0.02250	0.961	- 3.9
12	0.01269	0.529	0.02400	1.024	+ 2.4
13	0.01330	0.547	0.02430	1.038	+ 3.8
14	0.01370	0.566	0.2420	1.034	+ 3.4
15	0.01404	0.583	0.02410	1.030	+ 3.0
16	0.01437	0.600	0.02396	1.023	+ 2.3
17	0.01480	0.615	0.02408	1.029	+ 2.9
18	0.01474	0.628	0.02345	1.001	+ 0.1
19	0.01515	0.641	0.02364	1.010	+ 1.0
20	0.01535	0.652	0.02357	1.006	+ 0.6
21	0.01567	0.662	0.02370	1.012	+ 1.2
22	0.01572	0.668	0.02352	1.004	+ 0.4
23	0.01647	0.673	0.02446	1.044	+ 4.4
	0.28074				

note : uniform q = 0.2342 cfs/ft

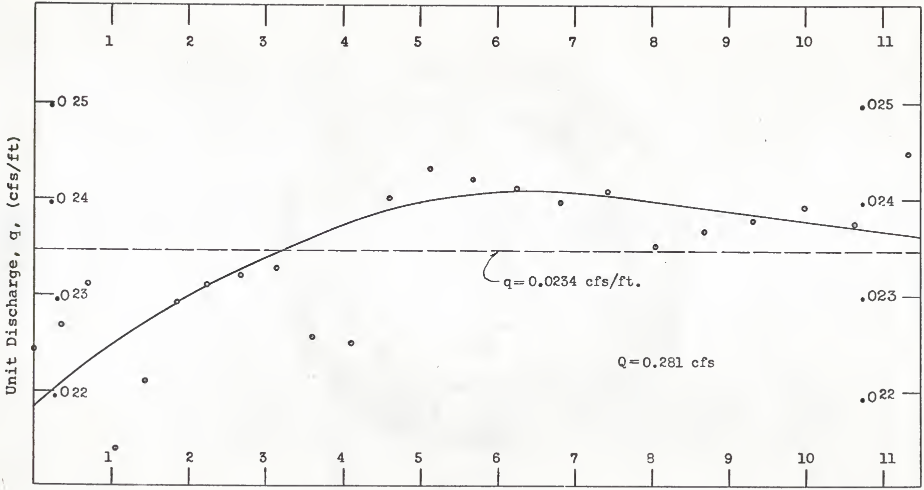

Length, L, ft

Fig, 21.

Discharge Distribution Curve

Table 9 $Q = 0.22076$ cfs, $h_b = 0.71$ ft, $h_d = 1.18$ ft, $h_c = 1.40$ ft.

port no.	q (cfs)	ΔL (ft)	uniformity: $q/\Delta L$ (cfs/ft)	uniformity: dimensionless uniformity	uniformity: % of deviation from uniform distribution
1	0.00620	0.334	0.01856	1.010	+ 1.0
2	0.00650	0.351	0.01850	1.005	+ 0.5
3	0.00690	0.367	0.01880	1.022	+ 2.2
4	0.00664	0.384	0.01730	0.930	- 7.0
5	0.00715	0.401	0.01782	1.032	+ 3.2
6	0.00763	0.417	0.01830	0.994	- 0.6
7	0.00797	0.435	0.01832	0.996	- 0.4
8	0.00830	0.453	0.01830	0.994	- 0.6
9	0.00870	0.473	0.01840	1.000	0.0
10	0.00870	0.492	0.01768	0.961	- 3.9
11	0.00904	0.511	0.01770	0.963	- 3.7
12	0.00980	0.529	0.01851	0.984	- 1.6
13	0.01030	0.547	0.01885	1.024	+ 2.4
14	0.01056	0.566	0.01865	1.014	+ 1.4
15	0.01080	0.583	0.01854	1.008	+ 0.8
16	0.01111	0.600	0.01852	1.007	+ 0.7
17	0.01140	0.615	0.01854	1.008	+ 0.8
18	0.01140	0.628	0.01819	1.011	+ 1.1
19	0.01170	0.641	0.01826	0.993	- 0.7
20	0.01200	0.652	0.01841	1.000	0.0
21	0.01230	0.662	0.01859	1.011	+ 1.1
22	0.01246	0.668	0.01863	1.012	+ 1.2
23	0.01320	0.673	0.01960	1.065	+ 6.5
	0.22076				

note : uniform q = 0.1840 cfs/ft.

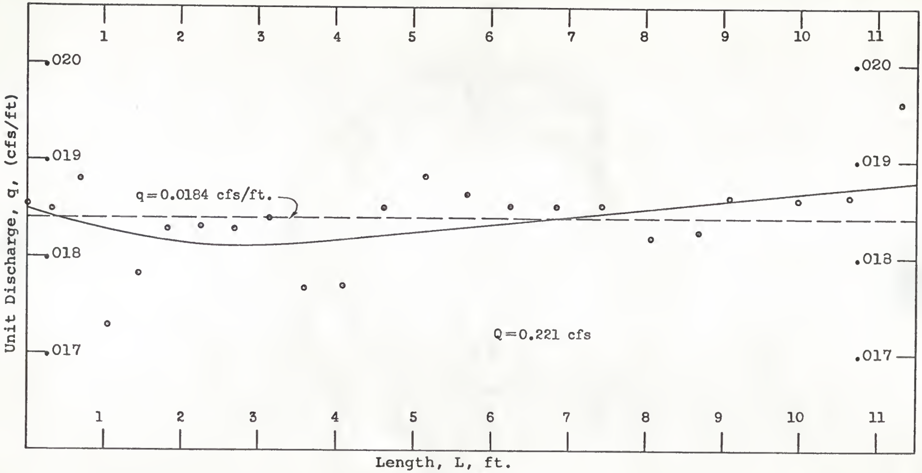

Fig. 22.

Discharge Distribution Curve

Table 10 $Q=0.1915$cfs, $h_b=0.540$ft, $h_d=0.872$ft, $h_c=1.026$ft.

port no	q (cfs)	ΔL (ft)	q/ΔL (cfs/ft)	uniformity: dimensionless uniformity	uniformity: % of deviation from uniform distribution
1	0.00563	0.334	0.01686	1.056	+ 5.6
2	0.00589	0.351	0.01680	1.052	+ 5.2
3	0.00620	0.367	0.01690	1.059	+ 5.9
4	0.00600	0.384	0.01561	1.021	+ 2.1
5	0.00634	0.401	0.01581	1.055	+ 5.5
6	0.00680	0.417	0.01630	1.022	+ 2.2
7	0.00703	0.435	0.01616	1.013	+ 1.3
8	0.00728	0.453	0.01609	1.009	+ 0.9
9	0.00760	0.473	0.01606	1.007	+ 0.7
10	0.00760	0.492	0.01544	0.969	- 3.1
11	0.00779	0.511	0.01525	0.958	- 4.2
12	0.00864	0.529	0.01597	1.002	+ 0.2
13	0.00891	0.547	0.01630	1.021	+ 2.1
14	0.00903	0.566	0.01604	1.006	+ 0.6
15	0.00924	0.583	0.01585	0.995	- 0.5
16	0.00951	0.600	0.01585	0.995	- 0.5
17	0.00973	0.615	0.01582	0.993	- 0.7
18	0.00970	0.628	0.01543	0.968	- 3.2
19	0.01004	0.641	0.01568	0.984	- 1.6
20	0.01023	0.652	0.01570	0.986	- 1.4
21	0.01053	0.662	0.01591	0.998	- 0.2
22	0.01070	0.668	0.01600	1.002	+ 0.2
23	0.01130	0.673	0.01680	1.052	+ 5.2
	0.19150				

note : uniform q = 0.1596 cfs/ft

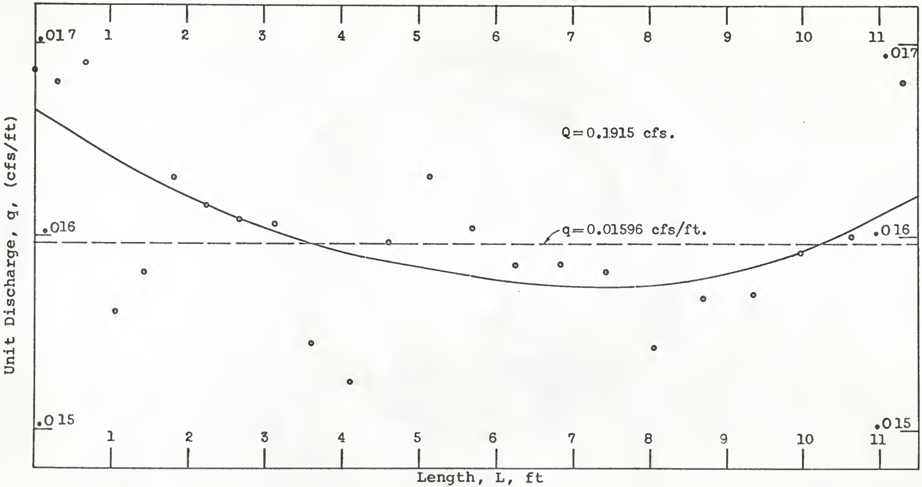

Fig. 23.

Discharge Distribution Curve

Table 11 $Q=0.16039 cfs$, $h_b=0.365 ft$, $h_d=0.607 ft$, $h_c=0.722 ft$.

port no.	q (cfs)	ΔL (ft)	q/ΔL (cfs/ft)	uniformity: dimensionless uniformity	uniformity: % of deviation from uniform distribution
1	0.00490	0.334	0.01466	1.097	+ 9.7
2	0.00515	0.351	0.01467	1.098	+ 9.8
3	0.00536	0.367	0.01460	1.092	+ 9.2
4	0.00513	0.384	0.01335	0.999	- 0.1
5	0.00541	0.401	0.01350	1.010	+ 1.0
6	0.00572	0.417	0.01370	1.025	+ 2.5
7	0.00591	0.435	0.01359	1.017	+ 1.7
8	0.00605	0.453	0.01336	1.000	0.0
9	0.00633	0.473	0.01337	1.000	0.0
10	0.00637	0.492	0.01293	0.967	- 3.3
11	0.00652	0.511	0.01275	0.953	- 4.7
12	0.00697	0.529	0.01316	0.984	- 1.6
13	0.00737	0.547	0.01346	1.007	+ 0.7
14	0.00750	0.566	0.01323	0.990	- 1.0
15	0.00760	0.583	0.01303	0.975	- 2.5
16	0.00781	0.600	0.01300	0.973	- 2.7
17	0.00802	0.615	0.01304	0.976	- 2.4
18	0.00802	0.628	0.01291	0.966	- 3.4
19	0.00831	0.641	0.01298	0.971	- 2.9
20	0.00852	0.652	0.01306	0.976	- 2.4
21	0.00880	0.662	0.01329	0.994	- 0.6
22	0.00897	0.668	0.01343	1.004	+ 0.4
23	0.00965	0.673	0.01434	1.073	+ 7.3
	0.16039				

note : uniform q = 0.01337 cfs/ft

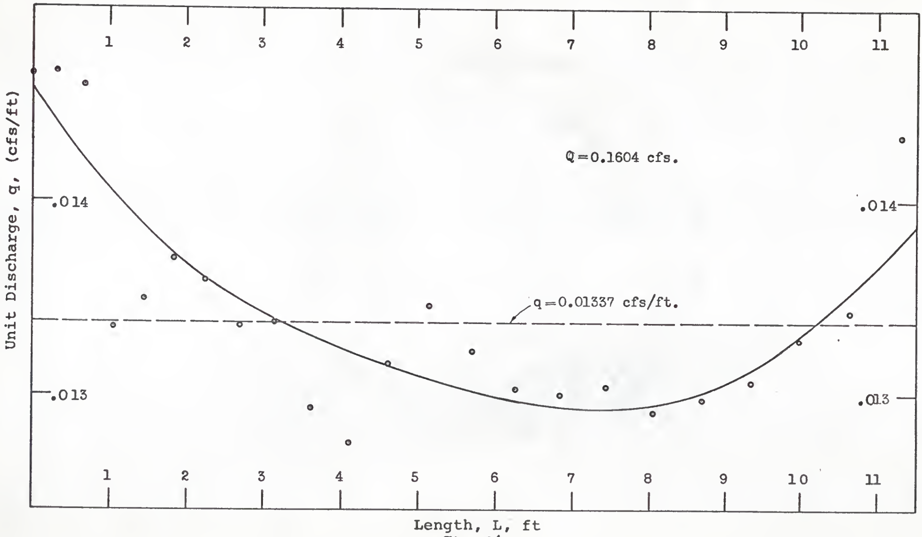

Fig. 24.

Discharge Distribution Curve

Table 12 $Q=0.13009cfs$, $h_b=0.211ft$, $h_d=0.362ft$, $h_c=0.445ft$.

port no.	q (cfs)	ΔL (ft)	$q/\Delta L$ (cfs/ft)	uniformity: dimensionless uniformity	uniformity: % of deviation from uniform distribution
1	0.00420	0.334	0.01257	1.159	+15.9
2	0.00430	0.351	0.01225	1.129	+12.9
3	0.00443	0.367	0.01206	1.111	+11.1
4	0.00421	0.384	0.01096	1.010	+ 1.0
5	0.00442	0.401	0.01102	1.016	+ 1.6
6	0.00466	0.417	0.01117	1.029	+ 2.9
7	0.00476	0.435	0.01095	1.009	+ 0.9
8	0.00491	0.453	0.01083	0.997	- 0.3
9	0.00510	0.473	0.01078	0.993	- 0.7
10	0.00506	0.492	0.01028	0.947	- 5.3
11	0.00516	0.511	0.01009	0.929	- 7.1
12	0.00557	0.529	0.01051	0.968	- 3.2
13	0.00583	0.547	0.01065	0.981	- 1.9
14	0.00594	0.566	0.01049	0.966	- 3.4
15	0.00607	0.583	0.01040	0.958	- 4.2
16	0.00624	0.600	0.01040	0.958	- 4.2
17	0.00642	0.615	0.01043	0.961	- 3.9
18	0.00647	0.628	0.01029	0.948	- 5.2
19	0.00674	0.641	0.01051	0.968	- 3.2
20	0.00693	0.652	0.01063	0.979	- 2.1
21	0.00724	0.662	0.01083	0.998	- 0.2
22	0.00742	0.668	0.01109	1.021	+ 2.1
23	0.00801	0.673	0.01189	1.096	+ 9.6
	0.13009				

note : uniform q = 0.01085 cfs/ft.

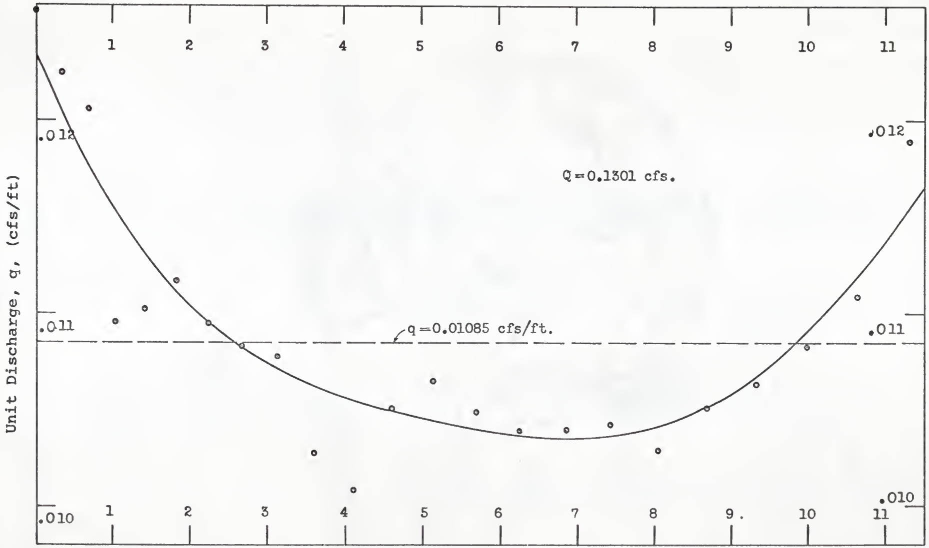

Fig. 25.

Discharge Distribution Curve

Table 13 $Q=0.10025$cfs, $h_b=0.088$ft, $h_d=0.169$ft, $h_c=0.213$ft.

port no.	q (cfs)	ΔL (ft)	uniformity: $q/\Delta L$ (cfs/ft)	uniformity: dimensionless uniformity	uniformity: % of deviation from uniform distribution
1	0.00305	0.334	0.00913	1.096	+ 9.6
2	0.00319	0.351	0.00908	1.090	+ 9.0
3	0.00334	0.367	0.00909	1.091	+ 9.1
4	0.00322	0.384	0.00838	1.006	+ 0.6
5	0.00335	0.401	0.00838	1.002	+ 0.2
6	0.00364	0.417	0.00873	1.048	+ 4.8
7	0.00374	0.435	0.00860	1.033	+ 3.3
8	0.00387	0.453	0.00854	1.026	+ 2.6
9	0.00405	0.473	0.00857	1.029	+ 2.9
10	0.00403	0.492	0.00819	0.983	- 1.7
11	0.00410	0.511	0.00803	0.964	- 3.6
12	0.00450	0.529	0.00851	1.022	+ 2.2
13	0.00466	0.547	0.00852	1.023	+ 2.3
14	0.00474	0.566	0.00838	1.006	+ 0.6
15	0.00485	0.583	0.00832	0.998	- 0.2
16	0.00496	0.600	0.00827	0.993	- 0.7
17	0.00506	0.615	0.00823	0.988	- 1.2
18	0.00503	0.628	0.00801	0.962	- 3.8
19	0.00517	0.641	0.00807	0.968	- 3.2
20	0.00525	0.652	0.00805	0.966	- 3.4
21	0.00536	0.662	0.00810	0.973	- 2.7
22	0.00541	0.668	0.00810	0.973	- 2.7
23	0.00568	0.673	0.00845	1.015	+ 1.5
	0.10025				

note : uniform q = 0.00835 cfs/ft.

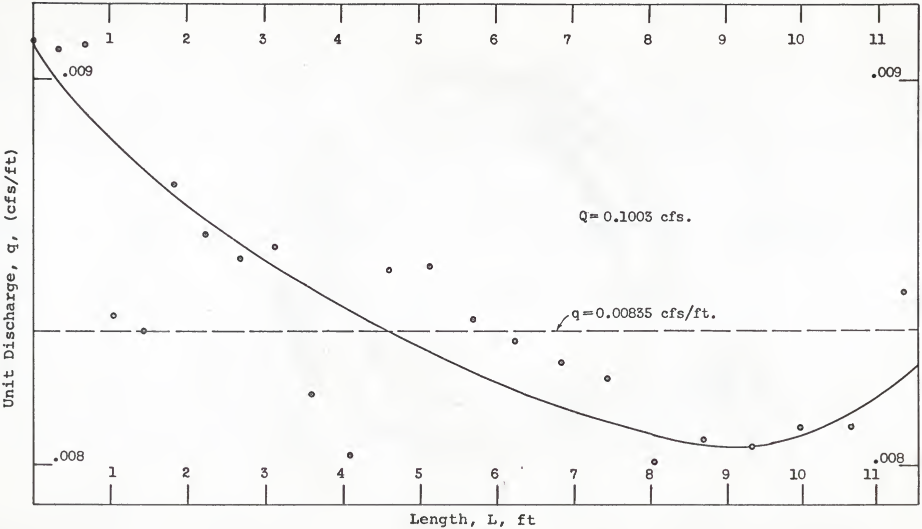

Fig. 26.

Discharge Distribution Curve

Table 14 $Q=0.07005cfs$, $h_b=0.021ft$, $h_d=0.083ft$, $h_c=01109ft$.

port no.	q (cfs)	ΔL (ft)	$q/\Delta L$ (cfs/ft)	uniformity: dimensionless uniformity	uniformity: % of deviation from uniform distribution
1	0.00155	0.334	0.00464	0.796	-20.4
2	0.00170	0.351	0.00485	0.832	-16.8
3	0.00183	0.367	0.00499	0.856	-14.4
4	0.00184	0.384	0.00479	0.822	-17.8
5	0.00200	0.401	0.00500	0.858	-14.2
6	0.00221	0.417	0.00530	0.909	- 9.1
7	0.00235	0.435	0.00541	0.928	- 7.1
8	0.00251	0.453	0.00554	0.950	- 5.0
9	0.00266	0.473	0.00563	0.966	- 3.4
10	0.00272	0.492	0.00553	0.948	- 5.2
11	0.00286	0.511	0.00560	0.960	- 4.0
12	0.00316	0.529	0.00598	1.026	+ 2.6
13	0.00338	0.547	0.00618	1.061	+ 6.1
14	0.00346	0.566	0.00611	1.048	+ 4.8
15	0.00359	0.583	0.00616	1.056	+ 5.6
16	0.00375	0.600	0.00625	1.071	+ 7.1
17	0.00385	0.615	0.00626	1.073	+ 7.3
18	0.00628	0.628	0.00610	1.047	+ 4.7
19	0.00397	0.641	0.00619	1.062	+ 6.2
20	0.00405	0.652	0.00622	1.067	+ 6.7
21	0.00416	0.662	0.00628	1.079	+ 7.9
22	0.00419	0.668	0.00627	1.075	+ 7.5
23	0.00443	0.673	0.00658	1.129	+12.9
	0.07005				

note : uniform $q = 0.0583$ cfs/ft

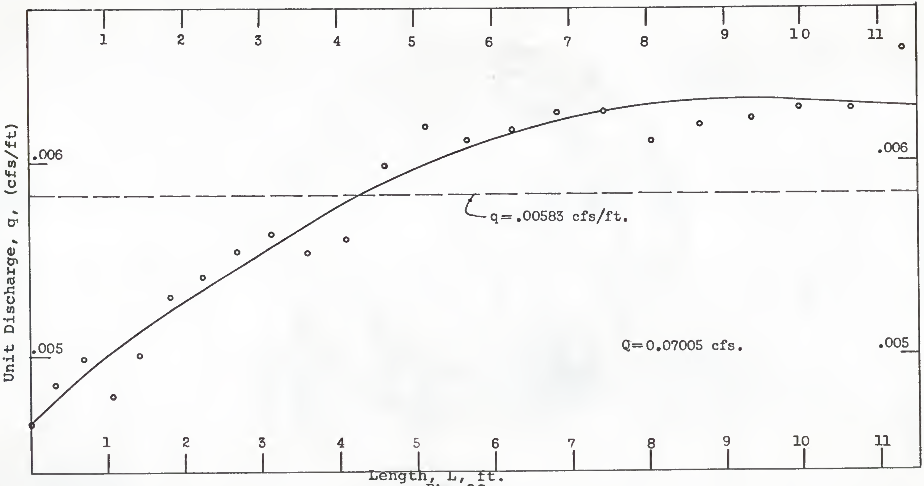

Fig. 27.

Discharge Distribution Curve

toward the closed end.

When Q = 0.221 cfs. it can be seen from table 9 and fig. 22, that the maximum q was 2.8% greater than the uniform q of 0.184 cfs/ft; the minimum q was 2.2% smaller than the uniform q. When Q was further reduced, this tendency to nonuniformity became more pronounced. When Q=0.195 cfs it is indicated by table 10 and fig. 23, that the maximum q was 4.5% greater than the uniform q of 0.01596 cfs/ft at the entrance, and the minimum q was 2.0% smaller than the uniform q at the mid-point of the manifold pipe.

When Q = 0.1604 cfs, table 11 and fig. 24 indicates that the maximum q was 9.1% greater than the uniform q of 0.1337 cfs/ft at the entrance and the minimum q was 3.5% smaller than the uniform q at the mid-portion of the manifold pipe.

When q=0.1301 cfs, according to table 12 and fig. 25 the maximum q was 14.7% greater than the uniform q of 0.01085 cfs/ft at the entrance, and the minimum q at the mid-portion of the manifold pipe was 4.7% smaller than the uniform q.

When Q was 0.1003 cfs, table 13 and fig. 26 indicates that the maximum q was 6.5% greater than the uniform q of 0.00835 cfs/ft. at the entrance and the minimum q at the mid-portion was 3.5% smaller than the uniform q. The last result indicates that the discharge per unit length seemed to return to a more uniform discharge distribution and this fact contradicts the former statement that when Q was further reduced, the tendency of nonuniformity would become pronounced. This contradiction might be explained by air entrainment in the fluid inside the main pipe. Since when Q was 0.1003 cfs h_b =0.088 ft., and h_b was measured from the centerline of the main pipe and since radius of the pipe was 0.0913 ft., hence h_b was smaller than the pipe radius, so that at the entrance of the manifold pipe, open channel flow occurred, so that air entrainment was forming. This phenomena affected the test result considerably. The same reasoning could be applied in explanation of the next test for Q=0.07 cfs, as it can be seen from table 14 and fig. 27, that q was much smaller at the entrance of the manifold pipe. The q was about 20% smaller at the entrance than the uniform q of 0.0583 cfs/ft, and increased gradually to 8.5% more than the uniform q in the end portion of the manifold pipe. When Q was 0.07 cfs, h_b was 0.021 ft, and h_d was 0.083 ft, indicating that open channel flow was presented over more than half the length of the manifold pipe and air entrainment would therefore be more serious. The uniformity characteristic, consequentely, would be of no interest.

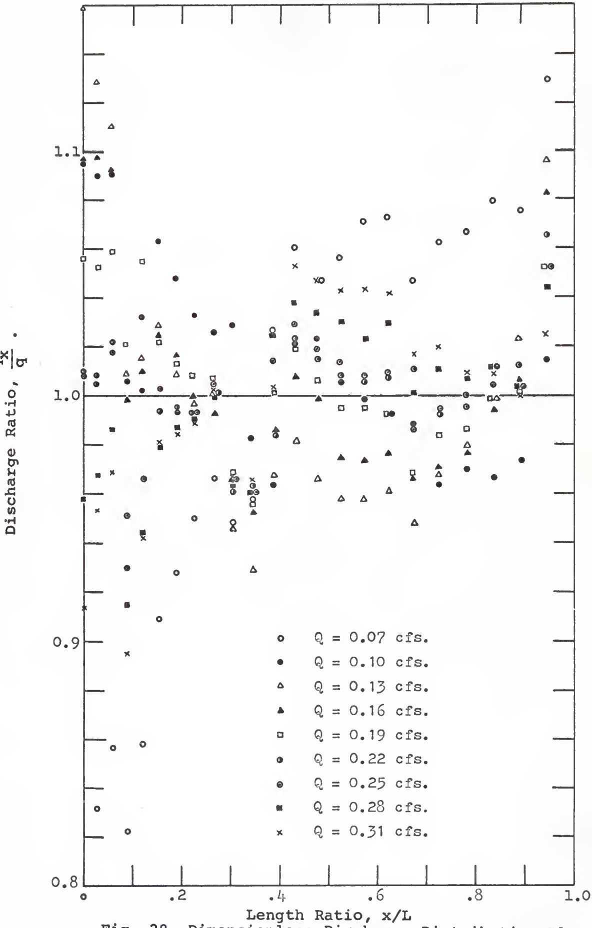

Fig. 28. Dimensionless Discharge Distribution Plot

CONCLUSIONS

In order to compare the uniformity characteristic of the manifold pipe flow at different discharges, the nine runs (i.e. with Q equal to 0.07, 0.10, 0.13, 0.16, 0.19, 0.22, 0.25, 0.28 and 0.31 cfs) were converted into dimensionless form and are plotted in fig. 28 which enables the reader to make the determination of the amount of deviation from the uniform value for various inflow rates. It is seen that when the inflow rate is different from the design discharge quantity, Q, of 0.25 cfs, then the manifold pipe experienced a nonuniform distribution of discharge along the length. When the inflow rate was greater than the design discharge quantity, Q, of 0.25 cfs, the tendency toward nonuniformity was much greater than when the inflow rate was smaller than the design Q.

In conclusion, when the allowable nonuniformity of discharge is ±5%, then the supplied Q must be limited to the range of approximately 0.2 cfs to 0.27 cfs, that is it should not exceed 8% more or 20% less than the design discharge. When the allowable nonuniformity of discharge is ± 10%, then the supplied Q must be limited to the range of approximately 0.16 cfs to 0.31 cfs, that is it should not exceed 24% more or 36% less than the designated discharge.

RECOMMENDATIONS FOR FURTHER RESEARCH

This thesis has set forth a method for designing a manifold pipe system with side flow discharge uniformly distributed along the length of main pipe. However, due to the interrelationship of a variety of geometric elements such as D, d, L, and n and flow conditions such as Q and h which were defined before, the manifold problem becomes a very complicated one. This thesis gives the design criterion for a PVC pipe with diameter D equal to 2.193 inches, port opening diameter, d, equal to 19/32 inches length, L, equal to 12 feet, and discharge, Q, equal to 0.25 cfs and closed end head h_c, equal to 1.667 ft.

Further research is need for the purpose of obtaining a more widely applicable design method for practical engineering design. A more extensive experiment with different flow conditions is recommended in order to set forth a more complete criterion or design chart to provide an engineer with an easy method for designing a manifold flow system.

As discussed before, the uniformity characteristics are a function of the ratios of total area of side ports, a, to the cross sectional area, A, of the main pipe. The ratio of the pipe diameter, D, to the active length, L, of the manifold pipe, which in this experiment was equal to 65.7 shoul be examined for a range of values. A range of values for $(\sum a)/A$, which in this experiment was equal to 1.71, should also be studied. Also a relationship between the spacing of side ports to $(\sum a)/A$ and L/D should be determined. These, of course, are out of the scope of this thesis.

ACKNOWLEDGMENT

The writer wishes to express his appreciation to Doctor Richard M. Haynie for his guidance and instruction given in the preparation of this thesis

REFERENCE

(1) Frederick A. Zenz,
"Minimize Manifold Pressure Drop,"
Hydrocarbon Processing & Petro Refiner, Vol. 41, Dec., 1962.

(2) John S. Mcnown & En-Yun Hsu,
"Application of Conformal Mapping to Divided Flow,"
First Midwest Conference on Fluid Dynamics, 1950. P. 150.

(3) W. E. Howland,
"Design of Perforated Pipe for Uniformity of Discharge,"
Third Midwest Conference on Fluid Mechanics Proceeding, 1953. P. 687.

(4) R. D. Glading,
"Loss of Head Determination in Uniformly Tapped Pipe,"
Engg. News Record, Vol. 125. P. 697.

(5) M. L. Enger & M. I. Levy,
"Pressure in Manifold Pipe,"
Journal of AWWA, Vol. 21, 1929.

(6) J. H. Horlock,
"An Investigation of The Flow in Manifolds with Open and Closed Ends,"
Journal of Aero Soc., Vol 60, 1956.

(7) A. Acrivos, B. D. Babcock & R. L. Pigford,
"Flow Distribution in Manifolds,"
Chemical Eng. Science, Vol. 10, 1959. P. 112.

(8) N. Malishewsky,
"Experiments in The Hydraulics of Filter Underdrains,"
Journal of AWWA, Vol. 17, 1927.

(9) J. D. Keller,
"The Manifold Problem,"
Journal of Applied Mech., Mar, 1949, Vol. 16, No.1. P.77.

(10) Andrew Vazsonyi,
"Pressure Loss in Elbows and Duct Branches,"
ASME Transactions, Vol. 66, 1944.

(11) John Allen & Brian Albinson,
"An Investigation of The Manifold Problem for Incompressible Fluid with Special Reference to The Use of Manifold for Canal Locks,"
ASCE Proceeding, 1955. P. 114.

APPENDIX

Appendix A Test data for the skin friction coefficient, f, of two inch PVC pipe. (See page 13 for related discussion.)

	Q (cfs)	Q^2	h_f (ft)	h_f/Q^2	f_*	N_{r**}
1	0.0362	0.001310	0.0545	41.60	0.02805	23,930
2	0.0358	0.001282	0.0538	41.90	0.02831	23,810
3	0.0345	0.001190	0.0505	42.30	0.02854	22,910
4	0.0378	0.001430	0.0600	41.90	0.02990	25,090
5	0.0390	0.001521	0.0622	40.80	0.02754	25,910
6	0.0401	0.001610	0.0633	38.30	0.02587	26,620
7	0.0382	0.001460	0.0612	41.90	0.02990	25,360
8	0.0371	0.001379	0.0578	42.00	0.02839	24,610
9	0.0357	0.001277	0.0528	41.40	0.02795	23,720
10	0.0340	0.001158	0.0505	43.60	0.02941	22,560
11	0.0325	0.001058	0.0455	43.00	0.02904	21,580
12	0.0319	0.001020	0.0438	41.90	0.02830	21,170
13	0.0304	0.000925	0.0405	43.80	0.02956	20,160
14	0.0286	0.000819	0.0367	44.80	0.03026	18,970
15	0.0257	0.000661	0.0317	48.00	0.03239	17,060
16	0.0238	0.000568	0.0267	47.00	0.03170	15,800
17	0.0219	0.000480	0.0250	53.10	0.03581	14,540
18	0.0188	0.000354	0.0190	53.70	0.03695	12,410
19	0.0155	0.000241	0.0133	55.20	0.03724	10,290
20	0.0140	0.000196	0.0117	59.90	0.04041	9,290
21	0.0061	0.000037	0.0035	95.10	0.06420	4,020
22	0.0081	0.000066	0.0053	80.00	0.05410	5,380
23	0.0393	0.001523	0.0590	36.12	0.02439	26,120
24	0.0479	0.002300	0.0813	35.38	0.02388	31,820

	Q (cfs)	Q^2	h_f (ft)	h_f/Q^2	f *	N_r **
25	0.0535	0.002870	0.1030	35.88	0.02422	35,520
26	0.0581	0.003380	0.1194	35.28	0.02384	38,600
27	0.0651	0.004240	0.1454	34.26	0.02315	43,240
28	0.0741	0.005500	0.1774	32.28	0.02181	49,190
29	0.0788	0.006220	0.2048	32.98	0.02226	54,200
30	0.0810	0.006580	0.2134	32.40	0.02189	53,800
31	0.0339	0.001148	0.0500	43.52	0.02940	22,520
32	0.0304	0.000924	0.0317	34.28	0.02314	20,200
33	0.0261	0.000681	0.0200	29.36	0.01981	17,340
34	0.0228	0.000519	0.0150	28.84	0.01945	15,160
35	0.0145	0.000210	0.0083	39.70	0.02682	9,640
36	0.0097	0.000094	0.0067	70.80	0.04780	6,440
37	0.0438	0.001919	0.0074	38.80	0.02616	29,090
38	0.0602	0.003620	0.0130	36.10	0.02438	40,000
39	0.0717	0.005130	0.0177	34.60	0.02336	47,600
40	0.0796	0.006330	0.0228	36.10	0.02438	52,800
41	0.0800	0.006400	0.0216	33.80	0.02279	53,200
42	0.0756	0.005700	0.0186	32.70	0.02207	50,200
43	0.0985	0.009690	0.0313	30.80	0.02078	65,500
44	0.0710	0.005030	0.0176	35.10	0.02372	47,180
45	0.0666	0.004430	0.0160	36.10	0.02439	44,220
46	0.0578	0.003340	0.0133	39.40	0.02662	38,400
47	0.0389	0.001511	0.0060	39.70	0.02680	25,810
48	0.0298	0.000890	0.0035	39.30	0.02656	19,800
49	0.0097	0.000094	0.0068	72.30	0.04880	6,480

	Q (cfs)	Q^2	h_f (ft)	h_f/Q^2	f *	N_{r} **
50	0.0107	0.000125	0.0087	69.30	0.0468	7,120
51	0.0115	0.000132	0.0084	63.60	0.0429	7,630
52	0.0172	0.000296	0.0157	53.10	0.0358	11,410
53	0.0207	0.000428	0.0213	49.80	0.0336	13,770
54	0.0230	0.000529	0.0268	50.70	0.0342	15,290

note : * : obtained from equation (11) ; $f = 6.75(10^{-3})(h_f/Q^2)$

**: obtained from equation (12) ; $N_r = 6.64(10^5)Q$

Appendix B   The test data for determining the discharge coefficient C_q of side port of the manifold pipe in terms of V_{i+1}/V_i.

	Q_i (cfs)	q (cfs)	$Q_{i+1}=Q_i-q$ (cfs)	$\frac{Q_{i+1}}{Q_i}$	h (ft)	$a\sqrt{2gh}$	$C_q = q/a\sqrt{2gh}$
1	0.0971	0.0025	0.0946	0.975	0.29	0.0085	0.294
2	0.0990	0.0038	0.0952	0.962	0.54	0.0115	0.331
3	0.1031	0.0051	0.0980	0.951	0.85	0.0144	0.355
4	0.1069	0.0054	0.1015	0.950	0.80	0.0140	0.386
5	0.1120	0.0049	0.1071	0.957	0.53	0.0114	0.428
6	0.1170	0.0062	0.1108	0.948	0.81	0.0141	0.440
7	0.1190	0.0060	0.1130	0.950	0.69	0.0130	0.460
8	0.1231	0.0055	0.1176	0.956	0.55	0.0116	0.474
9	0.1261	0.0076	0.1185	0.941	1.05	0.0160	0.476
10	0.1292	0.0067	0.1225	0.948	0.77	0.0137	0.489
11	0.1343	0.0081	0.1262	0.940	1.07	0.0162	0.501
12	0.1381	0.0069	0.1312	0.950	0.77	0.0137	0.505
13	0.1450	0.0072	0.1378	0.950	0.66	0.0127	0.515
14	0.1432	0.0067	0.1365	0.946	0.70	0.0131	0.512
15	0.1468	0.0082	0.1386	0.944	1.00	0.0156	0.527
16	0.1521	0.0089	0.1432	0.942	1.09	0.0163	0.546
17	0.1560	0.0097	0.1463	0.938	1.25	0.0175	0.556
18	0.1582	0.0108	0.1474	0.932	1.51	0.0192	0.562
19	0.1591	0.0108	0.1483	0.934	1.45	0.0188	0.575
20	0.1600	0.0121	0.1479	0.924	1.78	0.0209	0.579
21	0.1681	0.0105	0.1576	0.938	1.31	0.0179	0.585
22	0.1642	0.0118	0.1524	0.928	1.60	0.0198	0.507
23	0.1723	0.0113	0.1610	0.935	1.45	0.0188	0.602

	Q_i (cfs)	q (cfs)	$Q_{i+1}=Q_i-q$ (cfs)	$\frac{Q_{i+1}}{Q_i}$	h (ft)	$a\sqrt{2gh}$	$C_q = q/a\sqrt{2gh}$
24	0.1782	0.0152	0.1630	0.915	2.60	0.0252	0.604
25	0.1791	0.0136	0.1655	0.924	2.07	0.0225	0.606
26	0.1800	0.0145	0.1655	0.919	2.29	0.0237	0.611
27	0.1851	0.0138	0.1713	0.925	2.07	0.0225	0.615
28	0.1870	0.0152	0.1718	0.918	2.45	0.0245	0.620
29	0.1890	0.0169	0.1721	0.911	2.96	0.0269	0.627
30	0.1912	0.0159	0.1753	0.917	2.62	0.0253	0.629
31	0.1962	0.0143	0.1819	0.927	2.11	0.0227	0.631
32	0.1983	0.0181	0.1802	0.909	3.32	0.0285	0.634
33	0.1994	0.0211	0.1783	0.895	4.50	0.0332	0.636
34	0.2033	0.0188	0.1845	0.907	3.51	0.0293	0.641
35	0.2050	0.0205	0.1845	0.900	4.13	0.0318	0.645
36	0.0437	0.0055	0.0382	0.847	0.29	0.0085	0.650
37	0.0468	0.0053	0.0415	0.888	0.27	0.0081	0.654
38	0.0489	0.0051	0.0438	0.897	0.25	0.0078	0.652
39	0.0501	0.0054	0.0447	0.893	0.27	0.0081	0.665
40	0.0637	0.0088	0.0549	0.863	0.72	0.0133	0.662
41	0.0729	0.0091	0.0638	0.875	0.77	0.0137	0.662
42	0.0788	0.0100	0.0688	0.873	0.94	0.0152	0.668
43	0.0809	0.0146	0.0663	0.820	1.94	0.0218	0.669
44	0.0813	0.0125	0.0688	0.846	1.42	0.0187	0.669
45	0.0849	0.0121	0.0728	0.858	1.33	0.0181	0.670
46	0.0925	0.0153	0.0772	0.835	2.10	0.0227	0.675
47	0.0998	0.0157	0.0841	0.842	2.17	0.0231	0.681
48	0.1079	0.0194	0.0885	0.820	3.28	0.0284	0.683

	Q_i (cfs)	q (cfs)	$Q_{i+1}=Q_i-q$ (cfs)	$\frac{Q_{i+1}}{Q_i}$	h (ft)	$a\sqrt{2gh}$	$C_q = q/a\sqrt{2gh}$
49	0.1184	0.0236	0.0948	0.800	4.87	0.0246	0.683
50	0.1075	0.0225	0.0850	0.790	4.36	0.0327	0.689
51	0.1060	0.0241	0.0816	0.770	5.10	0.0354	0.682
52	0.1253	0.0265	0.0988	0.748	6.03	0.0385	0.688
53	0.0561	0.0153	0.0408	0.729	1.99	0.0221	0.693
54	0.0599	0.0174	0.0425	0.708	2.63	0.0254	0.686
55	0.0530	0.0150	0.0380	0.717	1.92	0.0217	0.690
56	0.0522	0.0189	0.0333	0.640	3.10	0.0276	0.686
57	0.0591	0.0225	0.0366	0.619	4.38	0.0328	0.696
58	0.0600	0.0259	0.0341	0.569	5.66	0.0373	0.696
59	0.0480	0.0221	0.0259	0.540	4.18	0.0320	0.690
60	0.0391	0.0199	0.0192	0.491	3.41	0.0289	0.690

Appendix C The calculation of h(as defined in fig. 13) for discharge, Q, equal to 0.15, 0.20, 0.30, and 0.35 cfs flowing in the 2 inch PVC pipe with uniform discharge along the length of the manifold pipe.

Table C-1 $Q = 0.15$ cfs.

i	$\frac{L-x}{L}$	Q_i	V_i	$\frac{V_i^2}{2g}$	N_r	f_x	Δh_f	Σh_f	Δh
20	-	-	-	-	-	-	-	-	-
19	.05	.0075	0.29	.0013	5,000	.0565	.0002	.0002	.0011
18	.10	.0150	0.57	.0051	10,000	.0389	.0007	.0009	.0042
17	.15	.0225	0.86	.0114	14,900	.0329	.0012	.0021	.0093
16	.20	.0300	1.14	.0203	19,900	.0289	.0020	.0041	.0163
15	.25	.0375	1.43	.0317	24,900	.0275	.0029	.0070	.0288
14	.30	.0450	1.72	.0458	29,900	.0259	.0039	.0109	.0349
13	.35	.0525	2.00	.0621	34,800	.0247	.0051	.0160	.0461
12	.40	.0600	2.29	.0815	39,800	.0241	.0065	.0225	.0590
11	.45	.0675	2.57	.1027	44,700	.0233	.0079	.0304	.0723
10	.50	.0750	2.86	.1273	49,700	.0227	.0095	.0399	.0874
9	.55	.0825	3.14	.1536	54,700	.0220	.0111	.0510	.1026
8	.60	.0900	3.43	.1820	59,700	.0215	.0129	.0639	.1181
7	.65	.0975	3.71	.2140	64,700	.0210	.0148	.0787	.1353
6	.70	.1050	4.00	.2485	69,700	.0205	.0168	.0955	.1530
5	.75	.1125	4.29	.2860	74,700	.0201	.0190	.1145	.1715
4	.80	.1200	4.57	.3243	79,700	.0198	.0212	.1357	.1886
3	.85	.1275	4.86	.3671	84,600	.0196	.0238	.1595	.2076
2	.90	.1350	5.14	.4097	89,600	.0194	.0262	.1857	.2240
1	.95	.1425	5.43	.4595	94,600	.0192	.0291	.2148	.2447
0	1.00	.1500	5.71	.5070	99,500	.0190	.0318	.2466	.2604

Table C-2 $Q = 0.20$ cfs

i	$\frac{L-x}{L}$	Q_i	V_i	$\frac{V_i^2}{2g}$	N_r	f_x	Δh_f	Σh_f	Δh
20	-	-	-	-	-	-	-	-	-
19	.05	.01	0.38	.0023	6,600	.0480	.0004	.0004	.0019
18	.10	.02	0.76	.0090	13,200	.0344	.0010	.0014	.0076
17	.15	.03	1.14	.0202	19,900	.0298	.0020	.0034	.0168
16	.20	.04	1.53	.0362	26,600	.0266	.0032	.0066	.0296
15	.25	.05	1.91	.0565	33,200	.0250	.0047	.0113	.0452
14	.30	.06	2.29	.0813	39,800	.0241	.0065	.0178	.0635
13	.35	.07	2.67	.1108	46,500	.0231	.0084	.0262	.0846
12	.40	.08	3.05	.1446	53,100	.0220	.0105	.0367	.1079
11	.45	.09	3.43	.1830	59,800	.0213	.0128	.0495	.1335
10	.50	.10	3.81	.2256	66,300	.0206	.0153	.0648	.1608
9	.55	.11	4.19	.2728	73,000	.0199	.0199	.0847	.1881
8	.60	.12	4.58	.3260	79,700	.0195	.0209	.1056	.2204
7	.65	.13	4.96	.3820	86,400	.0193	.0243	.1299	.2521
6	.70	.14	5.33	.4410	92,800	.0191	.0277	.1576	.2834
5	.75	.15	5.72	.5080	99,600	.0190	.0318	.1894	.3186
4	.80	.16	6.10	.5780	106,100	.0189	.0359	.2253	.3527
3	.85	.17	6.48	.6530	112,900	.0188	.0404	.2657	.3873
2	.90	.18	6.87	.7330	119,600	.0187	.0451	.3108	.4222
1	.95	.19	7.24	.8150	126,000	.0187	.0502	.3610	.4540
0	1.00	.20	7.63	.9050	132,800	.0186	.0554	.4164	.4896

Table C-3 $Q = 0.30$ cfs

i	$\frac{L-x}{L}$	Q_i	V_i	$\frac{V_i^2}{2g}$	N_r	f_x	Δh_f	Σh_f	Δh
20	-	-	-	-	-	-	-	-	-
19	.05	.015	0.57	.005	9,900	.0390	.0006	.0006	.0042
18	.10	.030	1.14	.020	19,900	.0298	.0020	.0026	.0177
17	.15	.045	1.72	.046	30,000	.0259	.0039	.0065	.0390
16	.20	.060	2.29	.081	39,900	.0240	.0064	.0129	.0679
15	.25	.075	2.86	.127	49,800	.0228	.0095	.0224	.1041
14	.30	.090	3.43	.182	59,800	.0214	.0128	.0352	.1468
13	.35	.105	4.00	.248	69,700	.0205	.0167	.0519	.1963
12	.40	.120	4.57	.324	79,500	.0200	.0213	.0732	.2508
11	.45	.135	5.14	.410	89,400	.0195	.0263	.0995	.3105
10	.50	.150	5.72	.508	99,500	.0190	.0318	.1313	.3767
9	.55	.165	6.29	.613	109,400	.0187	.0378	.1691	.4439
8	.60	.180	6.86	.730	119,400	.0184	.0443	.2134	.5166
7	.65	.195	7.43	.854	129,300	.0182	.0511	.2645	.5895
6	.70	.210	8.00	.993	139,200	.0180	.0589	.3234	.6696
5	.75	.225	8.58	1.141	149,200	.0179	.0675	.3909	.7501
4	.80	.240	9.15	1.297	159,100	.0179	.0764	.4673	.8297
3	.85	.255	9.72	1.463	169,000	.0178	.0858	.5531	.9099
2	.90	.270	10.29	1.638	179,000	.0178	.0959	.6490	.9890
1	.95	.285	10.86	1.826	188,900	..0177	.1065	.7555	1.0705
0	1.00	.300	11.43	2.021	198,800	.0177	.1177	.8732	1.1478

Table C-4   Q = 0.35 cfs

i	$\frac{L-x}{L}$	Q_i	V_i	$\frac{V_i^2}{2g}$	N_r	f_x	Δh_f	Σh_f	Δh
20	-	-	-	-	-	-	-	-	-
19	.05	.0175	0.67	.007	11,700	.0362	.0008	.0008	.0061
18	.10	.0350	1.34	.028	23,300	.0282	.0026	.0034	.0241
17	.15	.0525	2.00	.062	34,800	.0249	.0051	.0085	.0536
16	.20	.0700	2.67	.110	46,500	.0230	.0083	.0168	.0934
15	.25	.0875	3.35	.172	58,300	.0215	.0122	.0290	.1434
14	.30	.1050	4.00	.248	69,600	.0207	.0169	.0459	.2022
13	.35	.1225	4.67	.338	81,300	.0198	.0220	.0679	.2703
12	.40	.1400	5.33	.441	92,800	.0194	.0281	.0960	.3450
11	.45	.1575	6.00	.559	95,800	.0190	.0350	.1310	.4280
10	.50	.1750	6.68	.689	116,200	.0184	.0418	.1728	.5162
9	.55	.1925	7.33	.834	127,600	.0182	.0499	.2227	.6113
8	.60	.2100	8.00	.993	139,200	.0180	.0589	.2816	.7114
7	.65	.2275	8.67	1.165	150,800	.0179	.0686	.3502	.8148
6	.70	.2450	9.33	1.350	162,300	.0178	.0790	.4292	.9208
5	.75	.2625	10.00	1.552	174,000	.0177	.0904	.5196	1.0324
4	.80	.2800	10.68	1.761	185,800	.0177	.1025	.6221	1.1389
3	.85	.2975	11.33	1.979	197,000	.0176	.1146	.7367	1.2423
2	.90	.3150	12.00	2.235	209,000	.0176	.1295	.8662	1.3688
1	.95	.3325	12.69	2.490	220,900	.0176	.1441	1.0103	1.4797
0	1.00	.3500	13.34	2.753	232,200	.0176	.1596	1.1699	1.5831

THE UNIFORMITY OF DISCHARGE THROUGH MANIFOLD PIPE

by

S. CHIEU-HSIUNG CHUANG

B. S., National Taiwan University, 1961

A MASTER'S THESIS

submitted in partial fulfillment of the

requirement for the degree

MASTER OF SCIENCE

Department of Civil Engineering

KANSAS STATE UNIVERSITY
Manhattan, Kansas

1967

THESIS ABSTRACT

The uniform distribution of discharge may be obtained from a manifold pipe with side ports of equal size and equal spacing if the total area of the side ports is small in comparison to the cross sectional area of the main pipe and the pipe is of large diameter in comparison to the active length of the manifold pipe. However, from the economic point of view, the size of the main pipe must be as small as possible, while the side ports must be numerous and large in order to minimize the pressure drop through them. This thesis sets forth a method for determining the variation in size and in spacing of the ports to accomplish both economy and uniformity of discharge.

When the distribution of the discharge is uniform along the length of the manifold pipe, the pressure head distribution along the manifold pipe can be determined by theoretical analysis. If the size of the side port is assumed, and the pressure head at any point in the pipe is known side flow discharge at this point can be determined, since it is proportional to the square root of pressure head at the point. The corresponding required spacing between ports, which is inversely proportional to the side flow discharge, can be determined. The location of each side port being known, an experimental apparatus can be designed. The test results and their deviation from the theoretical value are presented and discussed.

The investigation involved experimental runs at several inflow rates. When the inflow rate was different from the design discharge quantity the manifold pipe experienced a non-uniform distribution along the length. When the inflow rate was greater than the design

discharge quantity, Q, the tendency to non-uniformity of discharge was much greater than when the inflow rate was less than the design discharge quantity, Q.

It was concluded that when the allowable non-uniformity is ± 5% of the uniform value the inflow value should not exceed 8% greater or, 20% less, than the designated discharge, and when the allowable non-uniformity is ± 10% of the uniform value the inflow rate should not exceed 24% greater, or 36% less, than the designated discharge.